Development/Plasticity/Repair

Sox21 Promotes Hippocampal Adult Neurogenesis via the Transcriptional Repression of the *Hes5* Gene

Satoru Matsuda,[1,2]* Ken-ichiro Kuwako,[1]* Hirotaka James Okano,[1] Shuichi Tsutsumi,[5] Hiroyuki Aburatani,[5] Yumiko Saga,[6] Yumi Matsuzaki,[1] Akinori Akaike,[3] Hachiro Sugimoto,[2,4] and Hideyuki Okano[1]

[1]Department of Physiology, Keio University School of Medicine, Shinjuku-ku, Tokyo 160-8582, Japan, Departments of [2]Neuroscience for Drug Discovery and [3]Pharmacology, Graduate School of Pharmaceutical Sciences and [4]World-Leading Drug Discovery Research Center, Kyoto University, Sakyo-ku, Kyoto 606-8501, Japan, [5]Genome Science Division, Research Center for Advanced Science and Technology, The University of Tokyo, Meguro-ku, Tokyo 153-8904, Japan, and [6]Division of Mammalian Development, National Institute of Genetics, Mishima, Shizuoka 411-8540, Japan

Despite the importance of the production of new neurons in the adult hippocampus, the transcription network governing this process remains poorly understood. The High Mobility Group (HMG)-box transcription factor, Sox2, and the cell surface activated transcriptional regulator, Notch, play important roles in CNS stem cells. Here, we demonstrate that another member of the SoxB (Sox1/Sox2/Sox3) transcription factor family, Sox21, is also a critical regulator of adult neurogenesis in mouse hippocampus. Loss of Sox21 impaired transition of progenitor cells from type 2a to type 2b, thereby reducing subsequent production of new neurons in the adult dentate gyrus. Analysis of the Sox21 binding sites in neural stem/progenitor cells indicated that the Notch-responsive gene, *Hes5*, was a target of Sox21. Sox21 repressed *Hes5* gene expression at the transcriptional level. Simultaneous overexpression of *Hes5* and *Sox21* revealed that Hes5 was a downstream effector of Sox21 at the point where the Notch and Sox pathways intersect to control the number of neurons in the adult hippocampus. Therefore, Sox21 controls hippocampal adult neurogenesis via transcriptional repression of the *Hes5* gene.

Introduction

Endogenous neural stem/progenitor cells (NS/PCs) continuously give rise to neurons in the adult dentate gyrus (DG) of the hippocampus (Gage 2000; Duan et al., 2008). The "adult neurogenesis" phenomenon comprises several stages, which are strictly regulated by distinct mechanisms (Kempermann et al., 2004); however, the transcriptional network that governs adult neurogenesis remains largely unknown. The SRY-box containing gene (Sox) family, which encodes High Mobility Group (HMG)-box transcription factors, is essential for CNS development and for maintaining adult neurogenesis (Lefebvre et al., 2007). Among the members of this family, Sox1/Sox2/Sox3 (SoxB1) is reported to suppress neuronal differentiation by maintaining NS/PCs in an undifferentiated state (Kan et al., 2004; Bani-Yaghoub et al., 2006; Wang et al., 2006). In addition, Sox2-positive cells in the adult DG are thought to be NS/PCs, which contribute to the production of new neurons (Suh et al., 2007). Our previous immunohistochemical study using antibodies against SoxB1 and Sox21 demonstrated restricted expression of Sox21 in neurogenic regions in both embryonic and adult mouse brains (Tada et al., 2007). The neurogenic potential of Sox21 was indicated in the chick embryonic spinal cord, where it counteracts the effects of SoxB1 (Sandberg et al., 2005). Thus, Sox21 could conceivably also be involved in the regulation of adult neurogenesis in mice.

The Notch signaling pathway is also important for the regulation of CNS development, as it controls the proliferation and cell fate decisions of NS/PCs via downstream effectors such as Hes and Hey (Lewis 1996; Lathia et al., 2008). Recently, the Notch pathway was identified as a key regulator of the neurogenic niche in adult brains (Breunig et al., 2007; Imayoshi et al., 2010; Lugert et al., 2010). Thus, understanding the modulation of Notch signaling during adult neurogenesis may facilitate better understanding of the entire mechanism of adult neurogenesis.

The present study used *Sox21*-deficient ($Sox21^{-/-}$) mice to examine the *in vivo* function of the transcription factor Sox21 during hippocampal adult neurogenesis. Moreover, as a first step to unveiling the gene network downstream of Sox21, the target genes of Sox21 were screened using chromatin immunoprecipitation (ChIP) sequencing. Sox21 transcriptionally repressed the expression of *Hes5*, a known target of Notch signaling. By repressing *Hes5*, Sox21 contributed to the cancelation of the undifferentiated status of NS/PCs and promoted neurogenesis. Thus, this study demonstrates a pivotal role for Sox21 in the regulation of adult neurogenesis.

Received Nov. 21, 2011; revised June 21, 2012; accepted July 17, 2012.

Author contributions: S.M., K.-i.K., H.J.O., H.A., A.A., H.S., and H.O. designed research; S.M., K.-i.K., and S.T. performed research; Y.S. and Y.M. contributed unpublished reagents/analytic tools; S.M. and S.T. analyzed data; S.M., K.-i.K., S.T., and H.O. wrote the paper.

This work was supported by grants from the Japan Society for the Promotion of Science (S.M.), the Japanese Ministry of Education, Culture, Sports, Science and Technology (H.O.), Funding Program for World-leading Innovative R&D on Science and Technology (H.O.), Solution-Oriented Research for Science and Technology (SORST) of the Japan Science and Technology Agency (H.O.), and the Bridgestone Corporation. The funders had no role in study design, data collection, data analysis, the decision to publish, or preparation of this manuscript. We are grateful to Dr. F. H. Gage (Salk Institute for Biological Studies) for providing AHP cells. We also thank H. Naka-Kaneda (RIKEN Yokohama Institute), C. Hara-Miyauchi (Tokyo Medical and Dental University), F. Ozawa, Y. Imaizumi, S. Suzuki (Keio University), and N. Kaneko (Nagoya City University) for their expert technical assistance, and S. Shibata, K. Kakumoto (Keio University), T. Sunabori (Juntendo University), S. Fukami (Nara Medical University), K. Sawamoto (Nagoya City University), and other members of the Okano laboratory for helpful discussions and encouragement.

*S.M. and K.-i.K. contributed equally to this work.

Correspondence should be addressed to Hideyuki Okano at the above address. E-mail: hidokano@a2.keio.jp.

DOI:10.1523/JNEUROSCI.5803-11.2012

 0270-6474/12/3212543-15$15.00/0

Materials and Methods

Animals. All animal care and treatment procedures were performed in accordance with institutional guidelines approved by the Experimental Animal Care Committee of the Keio University School of Medicine. Animals were housed in a room with a 12 h light/dark cycle and fed *ad libitum*. *Sox21*$^{-/-}$ mice were established as described previously (Kiso et al., 2009) and maintained on a C57BL6/J background. The following primers were used to determine genotypes: wild-type alleles, 5′-CTCA TCCTTCCTCCCTCCCG-3′ and 5′-CCAAGCCAGCGGACTCAGAG AC-3′; mutant alleles, 5′-CGATCACATGGTCCTGCTGGAGT-3′ and 5′-CCAAGCCAGCGGACTCAGAGAC-3′ (same primer as for the wild-type alleles). *Hes5*-NLS*lacZ* knock-in mouse brains were kindly provided by Dr. R. Kageyama (Kyoto University, Kyoto, Japan) (Imayoshi et al., 2010). Animals of both sexes were used in this study.

BrdU treatment. Proliferating cells in the DG were labeled by short- or long-term administration of BrdU as previously described (Sakaguchi et al., 2006). Briefly, for long-term labeling, mice were administered 1 mg/ml of BrdU via the drinking water for 2 weeks and killed 4 weeks after the last day of administration. For short-term labeling, mice were injected intraperitoneally with 50 mg/kg of BrdU (Sigma-Aldrich) three times at 3 h intervals and killed 3 h after the last injection. To analyze embryonic neurogenesis, mice were injected intraperitoneally with 200 mg/kg of BrdU at embryonic day 15.5 (E15.5) and killed 1.5 h after the injection or on postnatal day 7 (P7).

Histological analysis. Animals were perfused with 4% (w/v) paraformaldehyde (Nakalai Tesque) and the brains dissected, postfixed in 4% paraformaldehyde at 4°C overnight, and sliced into 50 μm sections using a vibratome (Leica). To detect BrdU incorporation, tissue sections were pretreated with 1N HCl at 37°C for 30 min. To detect Ascl1-positive cells, tissue sections were pretreated with ice-cold acetone for 1 min. The sections were preblocked with Tris-NaCl blocking buffer containing 0.3% Triton X-100 for 1 h at room temperature (PerkinElmer) and incubated with primary antibodies at 4°C overnight followed by Alexa Fluor-, HRP-, or biotin-conjugated secondary antibodies for 90 min at room temperature. The Vectastain Elite ABC kit (Vector Laboratories) and/or Tyramide Signal Amplification (TSA)-Red or TSA-Green (PerkinElmer) were used to visualize HRP- and biotin-conjugated antibodies. Nuclei were counterstained with Hoechst 33258 (10 μg/ml; Sigma-Aldrich, B2883) for 10 min at room temperature. To visualize the structures of the hippocampus and cerebellum at P7, sections were stained with 0.2% cresyl violet (Nissl staining).

Antibodies for immunohistochemistry. The following primary antibodies were used in this study: anti-βIII-tubulin (rabbit IgG; Covance, PRB-435P; 1:500), anti-glial fibrillary acidic protein (GFAP; rabbit IgG; DAKO, Z0334; 1:500), anti-GFAP (mouse IgG; Sigma-Aldrich, G3893; 1:200), anti-fatty acid binding protein 7 (FABP7; rabbit IgG; Millipore, AB9558; 1:250), anti-Sox21 (goat IgG; R & D Systems, AF3538; 1:100), anti-Sox2 (rabbit IgG; Millipore, AB5603; 1:200), anti-Sox1/(2)/3 (rabbit IgG; gift from Dr. H. Kondoh, Osaka University, Osaka, Japan; 1:5000) (Tanaka et al., 2004), anti-Nestin (mouse IgG; BD Biosciences/PharMingen, 556309; 1:200), anti-doublecortin (DCX; goat IgG; Santa Cruz Biotechnology, sc-8066; 1:100), anti- DCX (rabbit IgG; Abcam, ab18723; 1:100), anti-polysialylated neuronal cell adhesion molecule (PSA-NCAM; mouse IgMκ; gift from Dr. T. Seki, Tokyo Medical University, Tokyo, Japan; 1:200), anti-NeuN (mouse IgG; Millipore, MAB377; 1:100), anti-S100β (mouse IgG; Sigma-Aldrich, S2532; 1:200), anti-glutathione *S*-transferase π (mouse IgG; BD Biosciences/PharMingen, 610719; 1:200), anti-Brn2 (Santa Cruz Biotechnology, sc-6029; 1:100), anti-Tbr1 (rabbit IgG; gift from Dr. R. F. Hevner, University of Washington, Seattle, WA; 1:10,000), anti-Ascl1 (mouse IgG; BD Biosciences/PharMingen, 556604; 1:100), anti-Tbr2 (rabbit IgG; Abcam, ab23345; 1:200), anti-Ki67 (rabbit IgG; Abcam, ab15580; 1:3000), anti-GFP (rabbit IgG, Medical and Biological Laboratories, 598, 1:500; goat IgG, Rockland, 600-101-215, 1:500), anti-BrdU (rat IgG; Abcam, ab6326; 1:100), anti-lacZ (rabbit IgG, Cappel, 55976, 1:500; goat IgG, Cappel, 56028, 1:500), and normal IgG (rabbit IgG, Millipore, DAM1421465; goat IgG, Santa Cruz Biotechnology, sc-2028). Immunoreactivity was visualized using Alexa Fluor-conjugated secondary antibodies (Invitrogen; 1:250) and HRP- or biotin-conjugated secondary antibodies (Jackson ImmunoResearch; 1:250).

Cell culture. The adult rat hippocampal progenitor (AHP) cell line was established as described previously (Palmer et al., 1997). Cultures were maintained on poly-L-ornithine-coated (Sigma-Aldrich) and laminin-coated (Sigma-Aldrich) dishes in DMEM/F-12 (1:1; Invitrogen) supplemented with N2 (Invitrogen) and 40 ng/ml recombinant human FGF-2 from *Escherichia coli* (PeproTech).

Retrovirus preparation. To prepare the retrovirus vectors, a pMYs-*Sox21*-IRES-*Egfp* or pMYs-3×flag-*Hes5*-IRES-*Egfp* plasmid was constructed by inserting the mouse *Sox21* (NC_000080.5) or *Hes5* (NC_000070.5) fragments into a pMYs-IG backbone (Kitamura et al., 2003). The open reading frames of *Sox21* and *Hes5* were PCR amplified from the pcDNA/Sox21 vector (Ohba et al., 2004) and from a cDNA library of neurospheres derived from embryonic stem cells, respectively. The following primers were used for subcloning the cDNA: *Sox21*, 5′-ccgggatccgccaccATGTCCAAGCCTGTGGAC CACGTCAAGC-3′and5′-ccgctcgagTCATAGCGCGGCAGCGTAGGCCG CGGGGTAG-3′; *Hes5*, 5′-ccggaattcgccaccATGGCCCCAAGTACCGTG-3′ and 5′-ccgctcgagTCACCAGGGCCGCCAGAGG-3′. Underlined letters in the sequences represent the restriction sites used for subcloning. The gccacc sequence is the Kozak sequence. The pMY-*Sox21*-2A-3×flag-*Hes5*-IRES-*Egfp* construct was generated by subcloning the *Sox21* fragment without a stop codon (primer sequences: 5′-ccggtcgacgccaccATGTCCAAGCCTGTG GACCACGTCAAGC-3′ and 5′-ccgggatccTAGCGCGGCAGCGTAGGCC GCGGGGTAG-3′). The 2A sequence was a gift from Dr. T. Maeda (Central Institute for Experimental Animals, Kanagawa, Japan). The 3× FLAG tag sequence was derived from the p3× FLAG-CMV-7 plasmid (Sigma-Aldrich).

Retrovirus was produced by transient transfection of Plat-E cells (Kitamura et al., 2003) with retrovirus constructs using GeneJuice (Novagen) according to the manufacturer's instructions. The medium was changed 24 h after transfection, and the supernatants were harvested 72 h after transfection. To ensure efficient *in vitro* and *in vivo* infection, the viral particles were concentrated by centrifugation at 8000 rpm for 16 h and resuspended in HBSS (Invitrogen).

In vivo *viral infection.* A retrovirus suspension (1 μl) was stereotactically injected into the DG of the hippocampus (coordinates relative to bregma, 2.0 mm posterior, 1.5 mm lateral, and 2.3 mm ventral from the skull) of anesthetized 6-week-old C57BL6 wild-type mice (purchased from Nihon SLC). After 3, 21, or 28 d, the mice were transcardially perfused with PBS and 4% PFA, and the brains were subjected to immunohistochemical analyses. To analyze the phenotype of the infected cells, at least 20 GFP-expressing cells in the subgranular zone (SGZ) and granule cell layer (GCL) were observed from each individual mouse, and the percentage GFP+/NeuN+ cells among the total GFP+ cell population was calculated.

ChIP–quantitative PCR and ChIP sequencing. ChIP was performed as described previously (Kaneshiro et al., 2007; Wakabayashi et al., 2009) with some modifications. Briefly, for ChIP–quantitative PCR (qPCR), AHP cells were harvested, and genomic DNA was cross-linked using 1% formaldehyde overnight at 4°C. Cross-linking was terminated by the addition of 125 mM glycine, and the chromatin was sonicated using an Ultrasonic Disrupter (Tomy Digital Biology; 10% duty, output level 1) for 10 h at 4°C. The sonicated chromatin was incubated with anti-Sox21 or anti-Sox2 antibodies coupled to magnetic DynaBeads (Active Motif) overnight at 4°C. The beads were washed five times with NaCl buffer, once with LiCl buffer (Millipore, 20-156), and twice with Tris-EDTA buffer. After washing, the DNA bound to the beads was eluted in elution buffer (1% SDS, 0.1 M $NaHCO_3$) overnight at 65°C to remove cross-links and desalted using the QIAquick PCR purification kit (Qiagen). ChIP samples were analyzed by real-time PCR using SYBR Premix Ex Taq (TaKaRa Biotechnology, #R0041B) and the following primers: mouse *Hes5* proximal promoter, 5′-CTGGGAAAAGGCAGCATATTGAG-3′ and 5′-ACGCTAAATTGCCTGTGAATTG-3′; mouse *Hes5* distal promoter, 5′-GATCCTCTGAAAGGTACAGGAAGG-3′ and 5′-CTCACA CCATCCGACTTGAGTA-3′; rat *Hes5* proximal promoter, 5′-GAAGGG AAGAAGGGAGAGAAGG-3′ and 5′-ACGCTAAATTGCCTGTGAAT TG-3′; and rat *Hes5* distal promoter, 5′-GATCCTCTGAAAGGTACAGG AAGG-3′ and 5′-CTCACACCATCCGACTTGAGTA-3′.

For ChIP sequencing, neurosphere cultures from the forebrains of E11.5 mouse embryos were used as the cell source. The DNA was purified

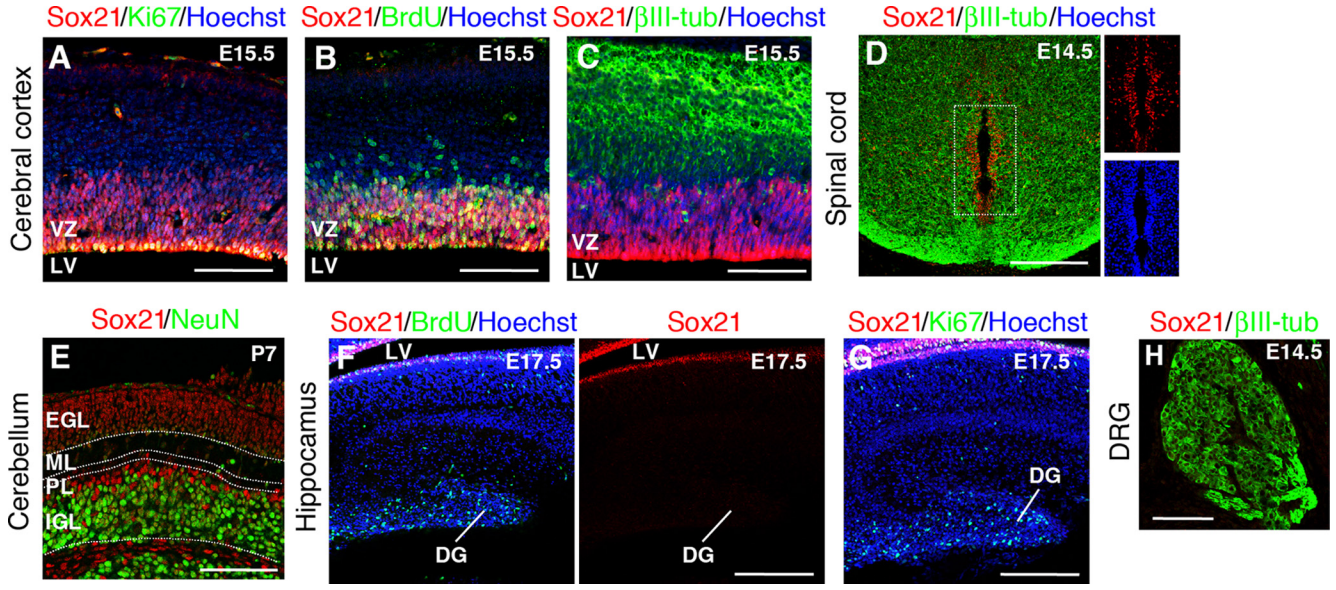

Figure 1. Expression of Sox21 in NS/PCs in the developing CNS. Immunohistochemical analyses of Sox21 in the mouse embryonic and postnatal nervous system. ***A–C***, E15.5 cerebral cortex. Sox21 was expressed in Ki67-positive (***A***) and BrdU-positive (***B***) proliferative NS/PCs in the VZ; expression was mutually exclusive with that of the neuronal marker βIII-tubulin (***C***). ***D***, E14.5 spinal cord. Sox21 was not expressed in βIII-tubulin-positive neurons. ***E***, P7 cerebellum. Sox21 was highly expressed in the EGL, and expression was mutually exclusive with that of the neuronal marker, NeuN. ***F***, ***G***, E17.5 hippocampus. BrdU- and Ki67-positive NS/PCs were observed; however, Sox21 was not expressed. ***H***, E14.5 dorsal root ganglia. Sox21 was not expressed in the DRG. Scale bars: ***A–C***, ***E***, ***H***, 100 μm; ***D***, ***F***, ***G***, 200 μm. VZ, Ventricular zone; LV, lateral ventricle; EGL, external granular layer, ML, molecular layer; PL, Purkinje cell layer; IGL, internal granular layer; DRG, dorsal root ganglia; DG, dentate gyrus.

from the ChIP eluates by SDS-PAGE to obtain ~100–300 bp fragments. Size-fractionated DNA was extracted, and a single adenosine was added using Exo-Minus Klenow DNA polymerase (3′ to 5′ exo-minus; Illumina). Illumina adaptors were then added, and the DNA was subjected to 20 cycles of PCR according to the manufacturer's instructions. The DNA was purified, and cluster generation and 36 cycles of sequencing were performed using the Illumina cluster station and 1G analyzer according to the manufacturer's instructions.

The sequence reads were obtained and mapped to the mouse [mm9; from the University of California, Santa Cruz (UCSC) database; http://genome.ucsc.edu] genomes using the Illumina Genome Analyzer Pipeline. As a result, 10,487,673 and 35,128,215 sequence reads were mapped uniquely for Sox21 and Sox2, respectively. For each 300 bp sliding window, the mapped sequence counts for ChIP were used for the calculation. The *p* value was also calculated, as the mapped sequences should follow a binominal distribution. The windows that passed the threshold and were located within 250 bp intervals were merged together and used for one binding site. For each binding site, the midpoint of the most significant (equal to the maximum $-\log_{10}p$) window was used as the peak position. To eliminate noise, regions containing >50% repetitive sequences (identified using RepeatMasker and simpleRepeats from the UCSC database) were discarded. Calculated *p* values were displayed using the Affymetrix Integrated Genome Browser.

Binding sites were compared using RefSeq and Known Genes from the UCSC database. Genes with binding sites within a region from 5 kb upstream to 1 kb downstream of their transcription start sites (TSSs) were annotated as bound genes. These analyses were performed using an in-house program written in Java.

De novo *computational analysis of consensus sequences.* MEME (Bailey and Elkan 1994) was used to search for enriched motifs among the binding sequences for both Sox21 and Sox2. Nonrepetitive sequences (repetitive rate, <10%; RepeatMasker and SimpleRepeats) of 200 bp around the position of the highest binding *p* values were used. The MEME program was applied to 495 sequences from the Sox21 ChIP data and 430 sequences from the Sox2 ChIP data. The motif generated for the matched sequences ($p < 10^{-5}$) was visualized using the WebLogo program (http://weblogo.berkeley.edu). The matrix score (0.0–1.0) was the highest score obtained using the position weight matrix method for each sequence (Kel et al., 2003).

Luciferase reporter analysis. To generate the reporter constructs, Venus-firefly luciferase (Luc) and/or a β-globin minimal promoter (pBG) fragment were introduced into the pGL3-basic vector (Promega). The *Hes5* genomic upstream regions (−2767 to +73 bp [distal regulatory element (DRE) and proximal promoter], −688 to +73 bp [proximal promoter], or −2767 to −2244 bp [DRE] from the TSS) of mouse genomic DNA were inserted into pGL3-Luc or pGL3-pBG-Luc vector. A point mutation in the Sox-binding sequence was introduced using a Mutagenesis kit (Sigma-Aldrich) and the following primers: 5′-CAGTGTTAAACGGCCCAAGCTTGCCAGGCGTG TGCCT-3′ and 5′-GGCCGTTTAACACTGTGAATGGGGCCAAAG-3′ (underlined letters indicate the mutated bases). The nucleotide sequences of these constructs were confirmed by DNA sequencing. Luc reporter constructs were cotransfected into AHP cells (80% confluent in 24-well plates) using expression vectors encoding *Sox21*, *Sox2*, and/or *Notch intracellular domain* (*NICD*; CMV-driven) and the FuGENE 6 transfection reagent (Roche). The amount of the reporter construct relative to the internal control vector was 12:1. Luc activity was assayed 24 h after transfection using a dual-luciferase reporter assay system (Picka-Gene Dual; Toyo Ink). A Renilla Luc vector driven by a TK promoter was used to normalize the transfection efficiency.

RNA extraction and RT-PCR. To isolate retrovirus-overexpressing AHP cells, cells were harvested 1.5 d after retroviral infection using 0.25% trypsin-EDTA, suspended in HBSS containing 10 mg/ml propidium iodide (PI), and filtered through a 30 μm mesh. The cells were sorted using a FACSVantage SE (Becton Dickinson) or a MoFlo Cell Sorter (Beckman Coulter), and viable infected cells (PI negative and GFP positive) were collected. To detect endogenous mRNA expression levels, hippocampal tissues from 6-week-old mice were dissected in cold PBS under a microscope using a scalpel. The cells or tissues were collected, and total RNA was isolated from GFP-sorted AHP cells or the hippocampus using TRIzol reagent (Invitrogen) and the Qiagen RNeasy Micro kit. cDNA was synthesized using Superscript III reverse transcriptase (Invitrogen). qPCR was performed in duplicate using SYBR green on a Stratagene MX3000P thermal cycler (Stratagene). The amount of cDNA was determined from the threshold cycle value after normalization with *gapdh* mRNA. Electrophoresis of all PCR products resulted in a single band of the correct size. Primer sequences were as follows: rat *Hes5*, 5′-ATGCTC AGTCCCAAGGAGAAAAAT-3′ and 5′-CAGGACTACAGCGAGGGTTA CTC-3′; mouse *Hes5*, 5′-AGAAAAACCGAGTAAGTGCAACTC-3′ and 5′-

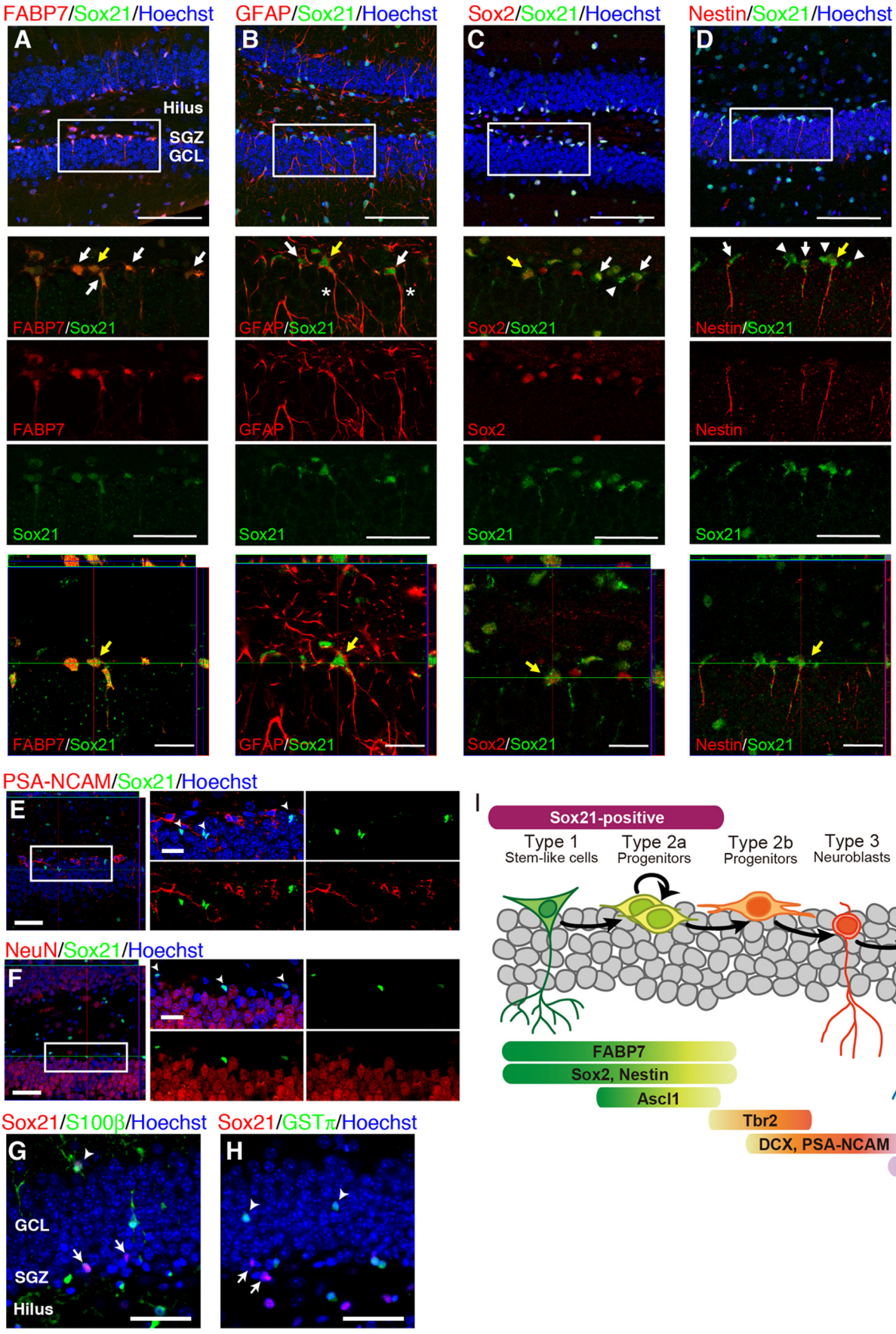

Figure 2. Specific expression of Sox21 in NS/PCs in the adult DG. Immunohistochemical analyses of Sox21 in the adult DG. ***A–D***, The areas surrounded by white rectangles in the top panels are shown in the magnified views in the middle three panels. Arrows indicate Sox21 and marker double-positive cells; arrowheads indicate Sox21 single-positive cells. The (*Figure legend continues.*)

CACCTTTGCTGTGTTTCAGGTAG-3′; and mouse/rat *Gapdh*, 5′-ACCA CAGTCCATGCCATCAC-3′ and 5′-TCCACCACCCTGTTGCTGTA-3′.

Knockdown of Hes5. The following four oligonucleotides were designed using the siDirect design program and used to knockdown mouse *Hes5* as *Hes5*-specific short hairpin RNAs: 5′-GCAGATGAAGCTGCTT TAA-3′, 5′-GATGCTCAGTCCCAAGGAA-3′, 5′-TCCTCCGCTAAGG CTGCTA-3′, and 5′-CCAGCGACACGCAGATGAA-3′. The pSilencer 2.1-U6 negative control (Ambion) sequence was used as a negative control. The efficiency and specificity of these sequences were evaluated by Western blotting of stable NIH3T3 transformants expressing mouse *Hes5* normalized to α-tubulin expression.

Western blotting. Western blotting was performed using standard protocols (Tada et al., 2007) with anti-Flag M2 (mouse IgG; Sigma-Aldrich, F3165; 1:1000) and anti-α-tubulin (mouse IgG; Sigma-Aldrich, T9026; 1:5000) antibodies. The blots were developed using ECL reagents (GE Healthcare) and the SuperSignal West Dura Extended Duration Substrate (Pierce).

Microscopy and quantification. To quantify the cell type of Sox21-positive cells in the adult DG, at least 20 Sox21+ cells in each mouse were detected, and the percentage of marker+/Sox21+ cells among the total Sox21+ cell population was calculated. Values were expressed as the mean ± SE ($n = 3$). For the quantitative analyses of marker coexpression, 1.5 μm sliced *z*-stacking images of at least five vibratome-cut coronal sections (50 μm thick) were analyzed in every sixth section using LSM510 and LSM700 confocal microscopes (Zeiss), and the numbers of cells double positive for stage-specific markers (FABP7, GFAP, Ascl1, Tbr2, DCX, or NeuN) and BrdU were counted. To quantify Sox2- and Ki67-positive cells in the P7 hippocampus, the number of immunopositive cells per 0.03 mm^2 DG was counted and expressed as cell number per mm^2 DG.

Results

Sox21 is expressed in NS/PCs in developing and adult nervous systems

We demonstrated previously the restricted expression of SoxB1 and Sox21 proteins in neurogenic regions in both embryonic and adult brains (Tada et al., 2007). To reveal the detailed expression pattern of Sox21 in the nervous system, we performed immunohistochemical analyses with antibodies directed against cell type markers and by BrdU labeling. Sox21 was exclusively expressed in the ventricular zone of the E15.5 cerebral cortex, which was populated by BrdU-incorporated and Ki67-positive NS/PCs but not βIII-tubulin-positive neurons (Fig. 1*A–C*). Similar Sox21 expression patterns were also observed in the NS/PC population in the E14.5 spinal cord and P7 cerebellum (Fig. 1*D*,*E*). In E17.5 hippocampus, however, Sox21 expression was not detected, even in BrdU-incorporated or Ki67-positive cells (Fig. 1*F*,*G*), which contrasted with the expression pattern of NS/PCs in the ventricular zone. Sox21 was not observed in E14.5 dorsal root ganglia (Fig. 1*H*).

We next examined the expression of Sox21 in the adult nervous system, particularly focusing on the hippocampus, which continuously generates new neurons. As we reported previously, Sox21 was expressed in the SGZ of the adult hippocampal DG (Tada et al., 2007) (Fig. 2). To further analyze the differentiation stage of Sox21-positive cells in the DG, immunohistochemical analyses using specific antibodies against Sox21 and cell-type-specific markers were performed. A large portion of Sox21-positive cells expressed FABP7 (73.2 ± 1.9%; Fig. 2*A*) and GFAP (81.6 ± 3.4%; Fig. 2*B*), both of which are markers for type 1 and 2a cells. Some Sox21-positive cells possessed radial glia-like fibers traversing the entire GCL (Fig. 2*B*, asterisks), a morphology typical of type 1 cells (Seri et al., 2001). Sox21 was also expressed in FABP7- or GFAP-positive cells in the hilus (Fig. 2*A*,*B*). Compared with FABP7 and GFAP, Sox21 expression showed less overlap with the other markers for type 1 and 2a cells, Sox2 (58.5 ± 9.4%; Fig. 2*C*), and Nestin (39.9 ± 4.5%; Fig. 2*D*). Sox21 was rarely coexpressed with PSA-NCAM, a marker for immature neurons (1.59 ± 1.59%; Fig. 2*E*), but was exclusively expressed with NeuN, a marker for mature neurons (Fig. 2*F*). In addition, Sox21 was not expressed in astrocytes (S100β positive) or oligodendrocytes (glutathione *S*-transferase π positive) in the adult DG or hilus (Fig. 2*G*,*H*). Together, these results indicated that Sox21 was expressed in a portion of type 1 stem-like cells and type 2a transient amplifying progenitors (Fig. 2*I*).

Adult neurogenesis, but not embryonic neurogenesis, is impaired in *Sox21*$^{-/-}$ mice

Because Sox21 was highly expressed in NS/PCs in both the embryonic and adult nervous systems (Fig. 1, 2), we next examined whether Sox21 plays a role in neurogenesis. To examine the function of Sox21 *in vivo*, *Sox21*-deficient/*GFP* knock-in (*Sox21*$^{-/-}$) mice (Kiso et al., 2009) were generated. In the P3 cerebral cortex of *Sox21*$^{-/-}$ mice, no obvious abnormality was detected in Brn2-expressing layer II–IV neurons and Tbr1-expressing layer VI neurons (Fig. 3*A*,*B*). Although Sox21 was highly expressed in the external GCL, which comprises precursor cells of granule neurons in P7 cerebellum (Fig. 1*E*), the thickness and cell density of the granule cell layer appeared normal in adult *Sox21*$^{-/-}$ cerebellum (Fig. 3*C*). Furthermore, consistent with the undetectable level of Sox21 expression in the embryonic hippocampus, the gross structure of the hippocampus was normal in P7 *Sox21*$^{-/-}$ mice (Fig. 3*D*). The numbers of Ki67- or Sox2-positive NS/PCs and NeuN-positive neurons that differentiated between the embryonic and neonatal stages were also not impaired in P7 *Sox21*$^{-/-}$ hippocampus (Fig. 3*E–G*). These results indicate that Sox21 may not play a crucial role in developmental neurogenesis in mice, at least in the regions that we analyzed.

We next examined the role of Sox21 in adult hippocampal neurogenesis using a well-established BrdU labeling strategy for the detailed analysis of adult neurogenesis in the subventricular zone and DG (Sakaguchi et al., 2006; Imaizumi et al., 2011). The long-term administration of BrdU followed by a 4 week washout period allows the retrospective analysis of the differentiation stage of BrdU-retaining cells (Fig. 4*A*). We first quantified the number of type 1 cells that retained BrdU, expressed FABP7 or GFAP, and also possessed radial glia-like fibers (which is a feature of type 1 cell morphology) in the SGZ in wild-type and *Sox21*$^{-/-}$ mice. As shown in Figure 4, *B* and *C*, the number of type 1 cells was not significantly changed in *Sox21*$^{-/-}$ mice. The number of proliferating type 1 cells that expressed Ki67 was also unchanged

←

(*Figure legend continued.*) cells highlighted by yellow arrows are also shown using orthogonal views at higher magnification in the bottom panels (top planes are through the *x-z* axes, and right planes are through the *y-z* axes). In the DG, Sox21 expression was restricted to cells in the SGZ. Sox21 was expressed in FABP7-positive (***A***) and GFAP-positive (***B***) NS/PCs with horizontally oriented cell bodies typical of type 2a cells and also in GFAP-positive stem-like cells with radial glia-like fibers (***B***, asterisk) typical of type 1 cells. ***C***, ***D***, The Sox21 expression pattern showed incomplete concordance with the other NS/PC markers, Sox2 (***C***) and Nestin (***D***). ***E***, Very few Sox21-positive cells coexpressed PSA-NCAM, a marker for immature neurons. Arrowheads indicate Sox21 single-positive cells. ***F***, The Sox21-positive cell population was mutually exclusive of NeuN-positive neurons in the DG. Arrowheads show Sox21 single-positive cells. ***G***, ***H***, Sox21 was not expressed in S100β-positive astrocytes or GSTπ-positive oligodendrocytes in the DG, although some S100β-positive cells outside the GCL (arrowhead) expressed Sox21. ***I***, A schematic summary of neuronal differentiation in the adult DG and the markers expressed at each stage. Scale bars: ***A–D***, top, 100 μm; middle, 50 μm; bottom, 20 μm; ***E***, ***F*** (panels with orthogonal views) ***G***, ***H***, 50 μm; ***E***, ***F*** (magnified views), 20 μm.

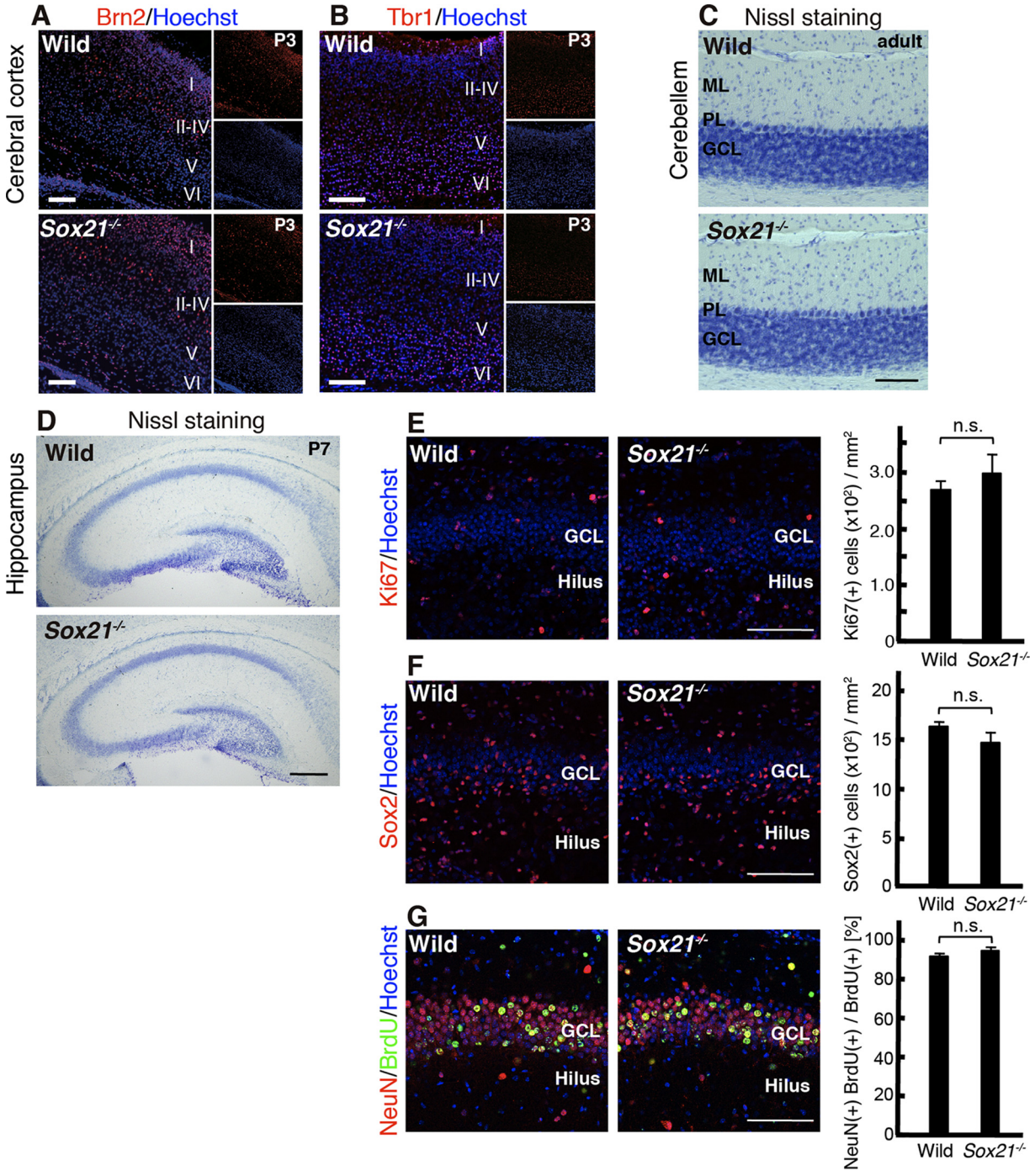

Figure 3. Normal neuronal development in *Sox21*$^{-/-}$ mice. ***A***, ***B***, Distribution of layer-specific neuronal markers in the cortex of wild-type and *Sox21*$^{-/-}$ mice at P3. Brn2 (layer II–IV; ***A***) and Tbr1 (layer VI; ***B***) expression patterns in *Sox21*$^{-/-}$ mice were similar to those in wild-type mice. ***C***, In the adult cerebellum, no impairment was observed in GCL thickness or the cell density in PL and ML. ***D***, The hippocampal structure was normal in P7 *Sox21*$^{-/-}$ mice. ***E***, ***F***, The numbers of Ki67-positive (***F***) and Sox2-positive (***F***) NS/PCs in the hippocampus were not altered in P7 *Sox21*$^{-/-}$ mice. ***G***, BrdU was administered at E15.5. BrdU-retaining NeuN-positive cells in P7 *Sox21*$^{-/-}$ mice were comparable with those in wild-type mice. Data represent the mean ± SE. n.s., No significance. Scale bars: ***A–C***, ***E–G***, 100 μm; ***D***, 300 μm. Abbreviations are as in Figure 1.

in *Sox21*$^{-/-}$ mice [0.38 ± 0.04 cells (wild type) vs 0.35 ± 0.06 cells (*Sox21*$^{-/-}$) per DG field; not significant; $n = 5$]. These results suggest that the deficiency of Sox21 did not influence the type 1 cell compartment.

To examine their efficiency for differentiating into neurons, we next compared the number of BrdU-retaining cells that expressed the immature neuronal marker DCX and the mature neuronal marker NeuN in wild-type and *Sox21*$^{-/-}$ mice. After the 4 week BrdU washout, the number of BrdU and NeuN double-positive cells was significantly reduced in *Sox21*$^{-/-}$ mice (Fig. 4*D*), while that of BrdU and DCX double-positive cells did not change (Fig. 4*E*), suggesting that deletion of *Sox21* impaired the generation of new neurons.

As the long-term BrdU treatment experiments showed that Sox21 deficiency resulted in fewer newly generated neurons without a defect in the type 1 stem cell population, the course of neuronal differentiation in *Sox21*$^{-/-}$ mice was likely impeded. Therefore, we next examined which differentiation stage was spe-

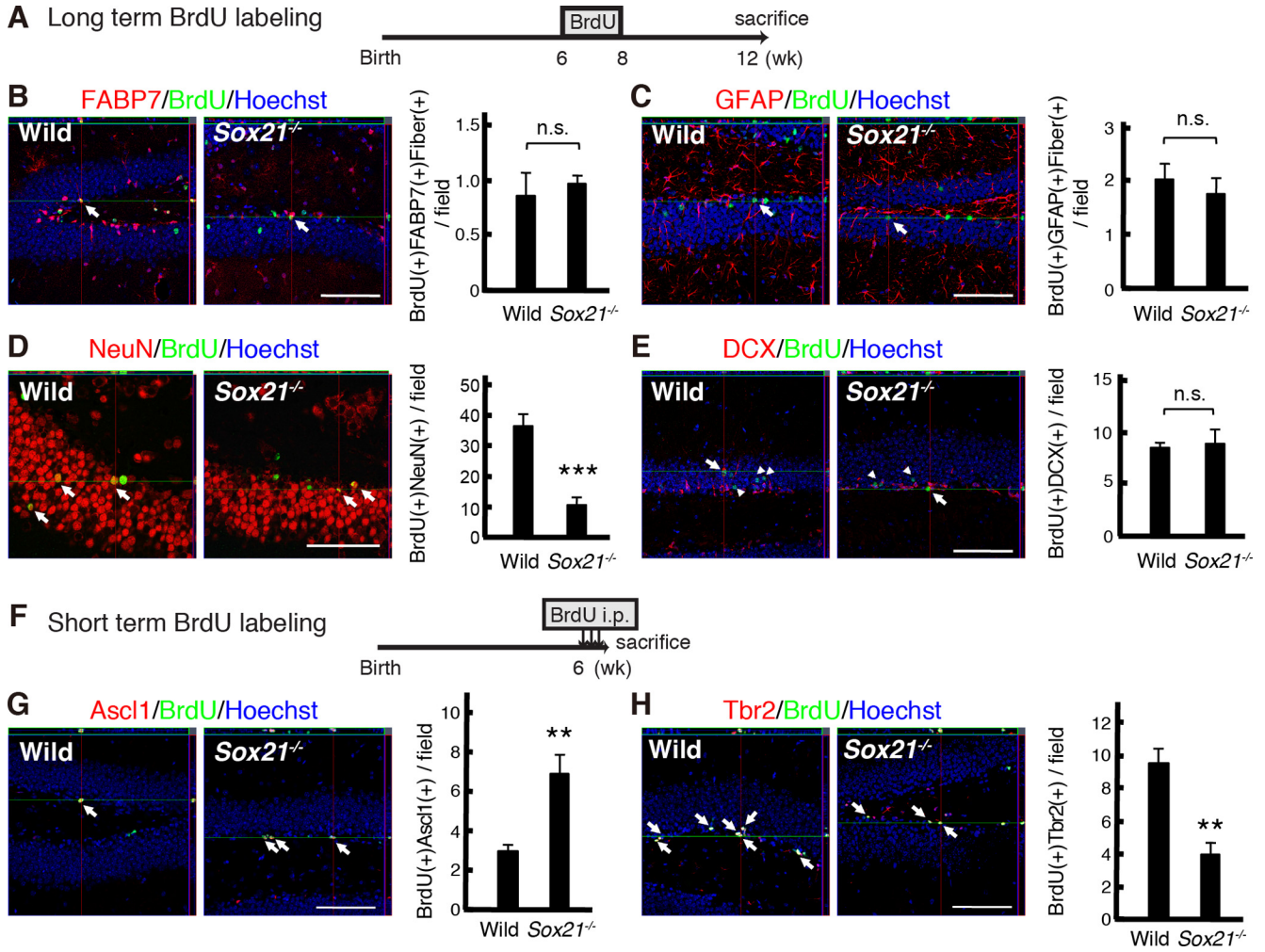

Figure 4. Impaired adult hippocampal neurogenesis in *Sox21*$^{-/-}$ mice. ***A***, Experimental scheme for long-term BrdU labeling analysis used to detect slowly dividing cells and neurons. ***B***, ***C***, To analyze type 1 cells, marker+/BrdU+/fiber+ cells (arrows) in wild-type and *Sox21*$^{-/-}$ mice were quantified 4 weeks after the last BrdU administration. The graphs show the numbers of FABP7+/BrdU+/fiber+ cells (***B***) and GFAP+/BrdU+/fiber+ cells (***C***) in the DG. ***D***, ***E***, To analyze newly generated mature and immature neurons, the numbers of BrdU+/NeuN+ (***D***) and BrdU+/DCX+ (***E***) cells were quantified 4 weeks after the last BrdU administration. ***F***, Experimental scheme for the short-term BrdU labeling analysis used to detect rapidly dividing cells. ***G***, ***H***, The number of BrdU+/Ascl1+ type 2a cells (***G***, arrows) increased, while the number of BrdU+/Tbr2+ type 2b cells (***H***, arrows) decreased, in *Sox21*$^{-/-}$ mice. The top planes are through the *x*–*z* axes, and the right planes are through the *y*-*z* axes. Data represent the mean ± SE. $^{**}p < 0.01$; $^{***}p < 0.001$ (two-sided *t* test). $n = 3$–5. n.s., No significance. Scale bars: 100 μm.

cifically impaired in *Sox21*$^{-/-}$ mice using a short-term BrdU treatment experiment (Fig. 4*F*) (Sakaguchi et al., 2006; Imaizumi et al., 2011). In this labeling protocol, the majority of BrdU-retaining cells are highly proliferative progenitors (type 2 cells), and the combination with immunostaining for cell-type-specific markers enables the progenitor population to be sorted into two stages. Neural progenitors in the former stage (type 2a) and the latter stage (type 2b) can be identified by their expression of Ascl1 (Kim et al., 2007) and Tbr2 (Hodge et al., 2008), respectively. In *Sox21*$^{-/-}$ mice, the number of BrdU and Ascl1 double-positive cells was significantly increased (Fig. 4*G*), while that of BrdU and Tbr2 double-positive cells was significantly decreased (Fig. 4*H*), suggesting that the loss of Sox21 caused the accumulation of type 2a cells and a reduction in type 2b cells. These results suggest that Sox21 may play a critical role in the transition of progenitors from type 2a to type 2b.

To directly confirm whether the impaired transition of progenitor stages in *Sox21*$^{-/-}$ mice impedes neuronal differentiation, we performed a genetic cell lineage tracing experiment. The *Gfp* gene was inserted into the *Sox21* gene locus in the mutant allele in heterozygous and homozygous mice (Kiso et al., 2009); hence, GFP-positive cells in *Sox21*$^{+/-}$ mice expressed Sox21 (Fig. 5*A*). Sox21 expression was completely abolished in *Sox21*$^{-/-}$ mice, and GFP-positive cells in the hippocampal SGZ represented *Sox21*-deficient cells (Fig. 5*B*). To assess the influence of *Sox21*-deficiency on progression to the neuronal stage in the adult DG, the cell fate of GFP-positive cells was investigated in *Sox21*$^{+/-}$ and *Sox21*$^{-/-}$ mice using the immature neuronal marker DCX. Although Sox21 protein itself was no longer expressed in immature neurons (Fig. 2*E*), due to the high stability of the GFP protein, a portion of the GFP-positive cells that progressed to the DCX-positive stage was detected in *Sox21*$^{+/-}$ mice (Fig. 5*C*, arrow). In contrast to *Sox21*$^{+/-}$ mice (Fig. 5*C*,*E*), most of the GFP-positive cells in *Sox21*$^{-/-}$ mice lacked significant DCX expression (Fig. 5*D*,*E*), confirming that *Sox21* deficiency results in impaired neuronal differentiation.

Together with the finding that Sox21 is mainly expressed in type 1 and type 2a cells (Fig. 2), the results of BrdU labeling experiments (Fig. 4) and the genetic cell lineage tracing experiment (Fig. 5) suggest that Sox21 plays an essential role in progenitor stage progression from type 2a to type 2b, thereby contributing to the generation of new neurons. As no abnormal-

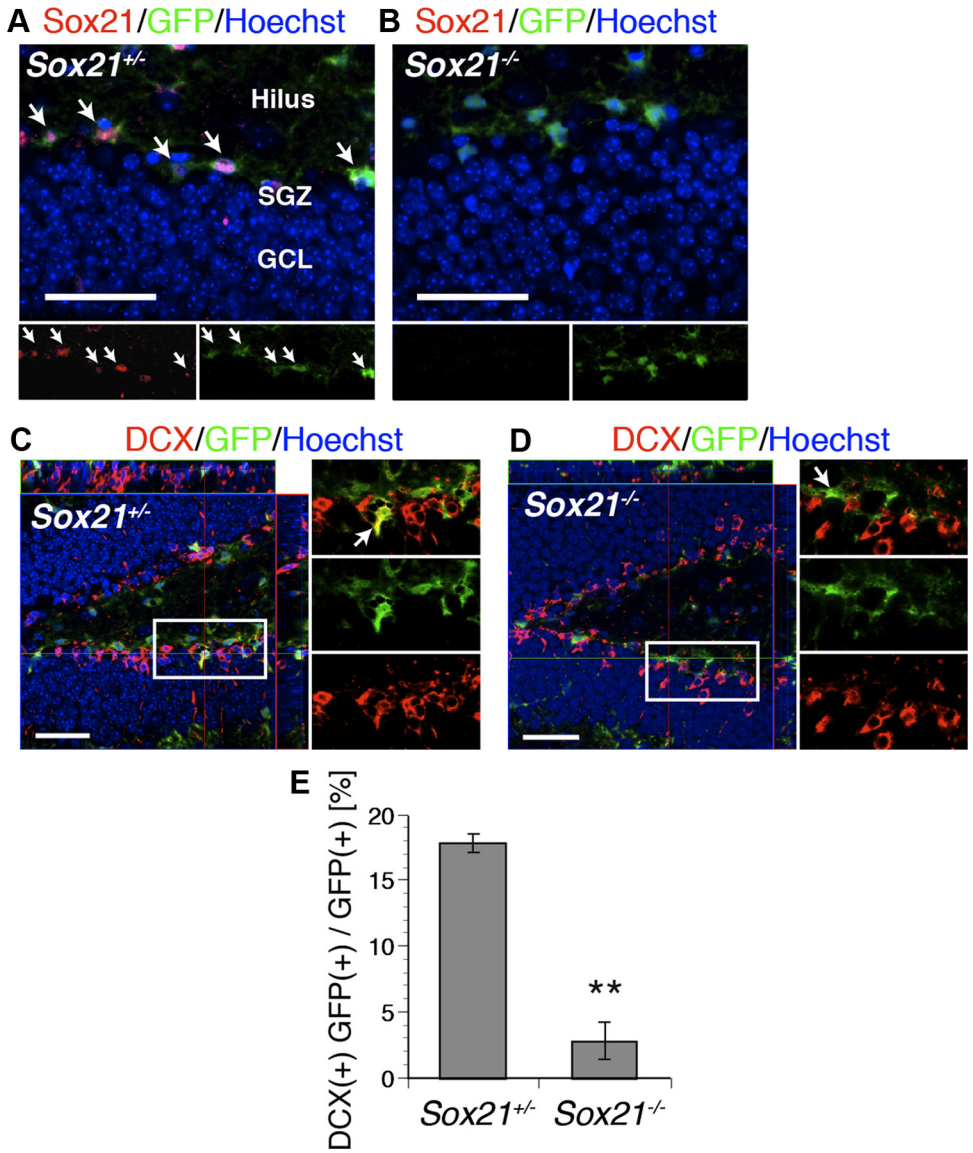

Figure 5. Lineage tracing analysis of Sox21-expressing and Sox21-deficient cells in the adult DG. ***A***, ***B***, GFP expression detected in the SGZ. ***A***, GFP was detected in all Sox21-positive cells (arrows) in *Sox21*$^{+/-}$ mice. ***B***, Sox21 expression was abolished in *Sox21*$^{-/-}$ mice. ***C***, ***D***, Double staining for GFP and the immature neuronal marker DCX. Top planes are through the *x-z* axes, and right planes are through the *y-z* axes. Magnified views are shown in the right panels. Some GFP+ cells (***C***, arrows) colocalized with DCX+ cells in *Sox21*$^{+/-}$ mice; however, GFP and DCX expression showed less overlap in *Sox21*$^{-/-}$ mice (***D***, arrows). ***E***, The proportion of DCX and GFP double-positive cells within the total GFP-positive cell population in the DG of *Sox21*$^{+/-}$ and *Sox21*$^{-/-}$ mice. Scale bars: 50 μm. Data represent the mean ± SE. $^{**}p < 0.01$ (two-sided *t* test). $n = 3$.

ities were detected in the neuron and NS/PC compartments in the neonatal *Sox21*$^{-/-}$ hippocampus (Fig. 3), the defect in adult neurogenesis in the *Sox21*$^{-/-}$ hippocampus is, conceivably, much less likely to be affected by developmental defects.

Sox21 overexpression promotes neuronal differentiation

To determine whether Sox21 is capable of promoting neuronal differentiation, a gain-of-function assay was performed *in vivo*. A retrovirus was stereotactically introduced into the DG of adult wild-type mice to induce expression of GFP and/or Sox21 in NS/PCs (Fig. 6*A*). Infection-derived GFP expression was restricted to the SGZ at 3 d after retrovirus infusion, which enabled monitoring of the fate of the NS/PCs (Fig. 6*B*). At 28 d after infusion of the retrovirus suspension, the majority of GFP-positive infected cells were found to reside in the GCL and SGZ (Fig. 6*C*,*D*). Among the control virus-infected cells, 11.5 ± 1.5% of the GFP-positive cells expressed the neuronal marker NeuN, while a significantly larger proportion (60.0 ± 5.9%) of GFP-positive cells in the Sox21-overexpressing group expressed NeuN (Fig. 6*F*). These results strongly support the hypothesis that Sox21 is an important positive regulator of the neuronal differentiation of NS/PCs in the adult DG.

The *Hes5* gene is a direct target of Sox21

To elucidate the molecular mechanism underlying Sox21-mediated regulation of neurogenesis, ChIP sequencing was performed using embryonic NS/PC cultures to identify the target genes of Sox21 and Sox2. Neurosphere cultures from the forebrains of embryonic mouse embryos at E11.5 were used as the cell source, because a large homogenous cell population was required to perform ChIP sequencing. After sequencing all genomic DNA that bound to endogenous Sox21 or Sox2 proteins, 284 regions from the Sox21-ChIP sequencing data and 301 regions from the Sox2-ChIP sequencing data were identified by comparison with

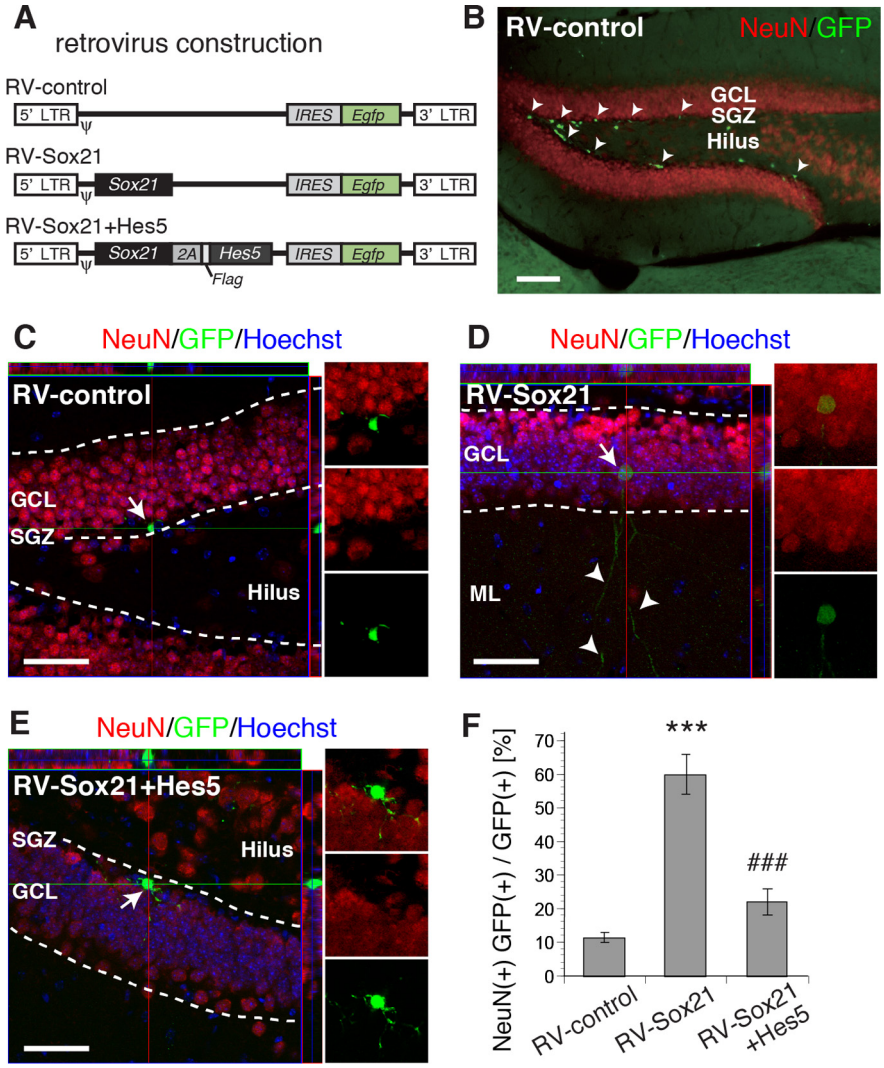

Figure 6. *Sox21* overexpression promoted neuronal differentiation of newborn cells *in vivo*. ***A***, Schematic showing control-, *Sox21*-, and *Sox21*-2A-*Hes5*-overexpressing retroviral (RV) constructs. ψ depicts a packaging signal used to generate the retrovirus. 2A depicts self-cleaving 2A peptides originating from the foot-and-mouth disease virus. ***B***, Micrographs of GFP-positive cells 3 d after retrovirus infusion into the DG of 6-week-old wild-type mice. The retrovirus infused into the DG delivered its transducing *GFP* gene selectively into NS/PCs in the SGZ of the hippocampus (arrowheads). ***C–E***, Micrographs showing retrovirus-labeled GFP-positive newborn cells (arrows) 28 d after retrovirus infusion into the DG of 6-week-old wild-type mice in the the controls (***C***), the *Sox21*-overexpressing group (***D***), and the *Sox21*-2A-*Hes5*-overexpressing group (***E***). The GFP-positive infected cell in ***D*** represents a mature granule neuron showing NeuN expression and long branches (arrowheads) in the ML of the hippocampus, whereas the majority of GFP-positive cells in the SGZ in ***C*** and ***E*** lacked NeuN expression and exhibited horizontally expanding branches typical of NS/PCs. ***F***, Quantification of neuronal differentiation in GFP-positive cells. The data represent the proportion of NeuN-positive cells within the total GFP-positive infected cell populations in the SGZ and GCL. Data represent the mean ± SE. $^{***}p < 0.001$; $^{\#\#\#}p < 0.001$ (two-sided *t* test). $n = 6–8$). Scale bars: ***B***, 100 μm; ***C–E***, 50 μm.

the input DNA sequencing data. Among them, 97 genomic loci were bound by both Sox21 and Sox2, which accounted for 34.5 and 32.2% of the regions bound by Sox21 and Sox2, respectively (Fig. 7*A*). The genes in which TSSs resided near the *p* value peak were then selected as the candidate targets (40 example target genes are listed in Table 1).

Among the candidate target genes of Sox21 and Sox2, the *Hes5* gene, encoding *Hairy and enhancer of split 5* (Akazawa et al., 1992), which acts as a downstream effector of Notch signaling, was selected because it contains Sox-consensus sequences (Fig. 7*B*) and maintains the undifferentiated state of NS/PCs and represses their neuronal differentiation (Ohtsuka et al., 1999). Sox21 and Sox2 bound to the *Hes5* gene at −312 to +10 bp from the TSS (Fig. 7*C*,*D*, bottom sequence). This area is highly conserved among various species and exhibits promoter activity for *Hes5* gene expression (Takebayashi et al., 1995). The maximum *p* values ($-\log_{10}p$) for Sox21 and Sox2 were 79.8 and 33.0, respectively. Surprisingly, another Sox21 binding site (maximum $-\log_{10}p = 73.4$) was identified at −2576 to −2335 bp from the TSS (Fig. 7*D*, top sequence). This region is also evolutionarily conserved but demonstrated no notable signal in the Sox2-ChIP sequencing data. Because the two regions covered by Sox21 contained the CBF/Suppressor of Hairless/Lag1 (CSL)- and Sox-consensus sequences (Fig. 7*D*), both regions may be involved in transcriptional regulation. In subsequent experiments, these regions were defined as a well-known proximal promoter and a novel DRE.

Because the ChIP sequencing data shown here were obtained from cultured embryonic NS/PCs, ChIP–quantitative PCR analyses were also performed using an AHP cell line (Palmer et al., 1997) to validate the occupation of the *Hes5* gene upstream regions by Sox21 and/or Sox2 in "adult"-type NS/PCs. The results were very similar to those obtained from ChIP sequencing using embryonic NS/PCs. Sox21 bound to both the proximal promoter and DRE, whereas Sox2 only bound to the proximal promoter in AHP cells (Fig. 7*E*). Thus, the results of the ChIP sequencing and ChIP–quantitative PCR analyses suggest that the *Hes5* gene may be a potential target of Sox21 in adult NS/PCs.

Sox21 represses *Hes5* expression in adult NS/PCs

The effect of Sox21 on *Hes5* gene promoter activity was analyzed using reporter experiments. The *Hes5* upstream genomic region (−2767 to +73 bp from the TSS) containing the proximal promoter and DRE was cloned into luciferase reporter plasmids and transfected with vectors carrying *NICD* or *Sox21* into AHP cells. NICD-induced *Hes5* promoter-luciferase activity was reduced by Sox21 coexpression in a dose-dependent manner (Fig. 8*A*, open columns). Intriguingly, introducing a mutation into the Sox21-binding sequence in the DRE (Fig. 8*A*, closed columns) completely canceled the repressive effect of Sox21. Furthermore, the repressive effect of Sox21 was mediated entirely by the DRE alone (−2767 to −2244 bp from TSS; Fig. 8*C*), and Sox21 did not affect luciferase activity by binding to the *Hes5* proximal promoter (−688 to +73 bp from the TSS; Fig. 8*B*). These results strongly suggest that Sox21 directly represses *Hes5* expression by binding to the DRE. We then investigated whether Sox2 competed with Sox21 to regulate *Hes5*. Although both Sox21 and Sox2 were capable of binding to the *Hes5* promoter, in sharp contrast to

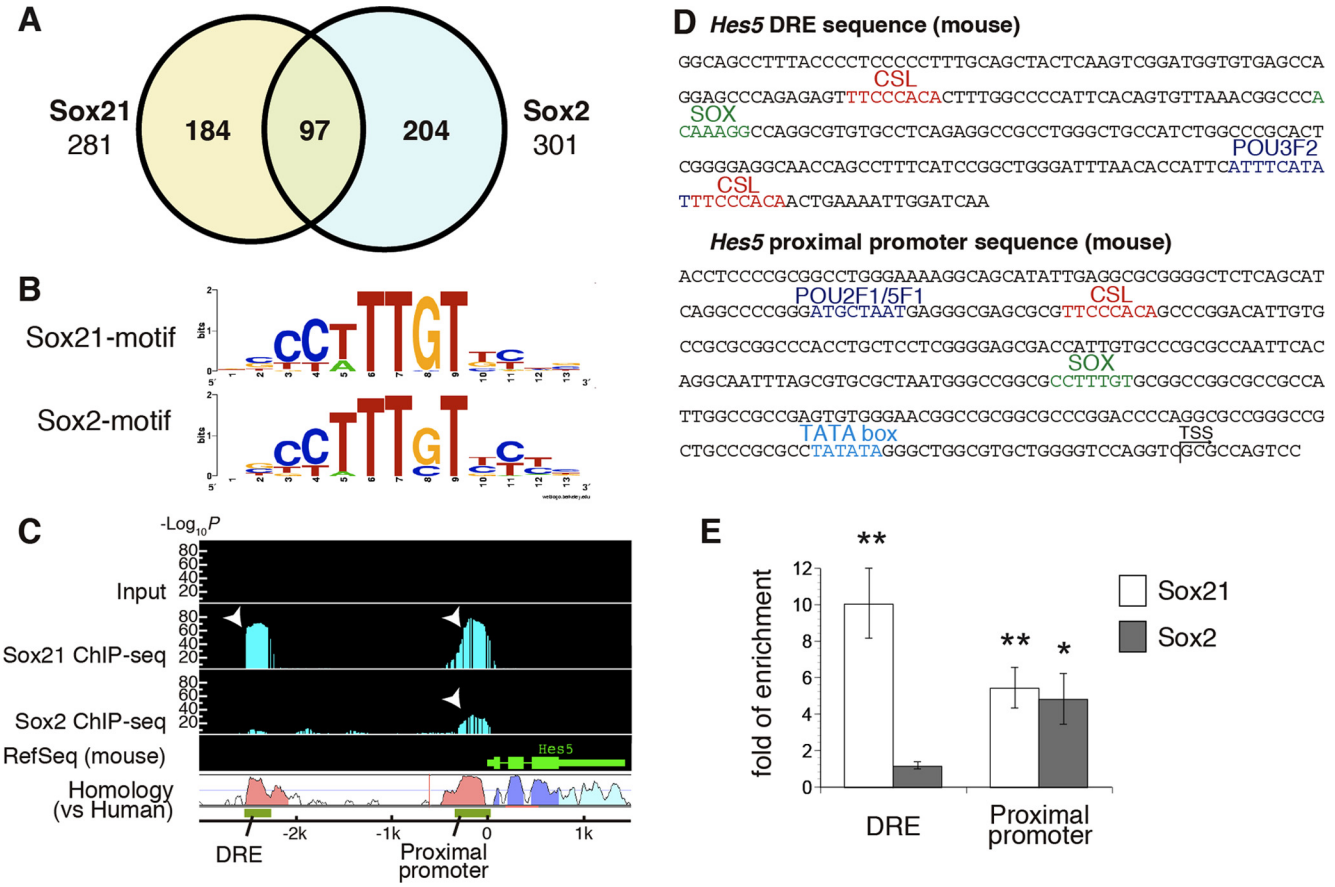

Figure 7. Identification of the *Hes5* gene as a target of Sox21 using ChIP sequencing analysis. ***A***, Venn diagram showing the number of genomic loci bound by Sox21 and Sox2. Of all the binding sites, 97 common genomic loci were bound by both Sox21 and Sox2. ***B***, Enriched motifs in Sox21- and Sox2-binding sequences identified by *de novo* computational analysis of ChIP sequencing data. The height of each character represents the relative frequency of the nucleotide appearance in the binding motifs. ***C***, Genomic view of the ChIP sequencing data around the *Hes5* gene. Binding by Sox21 and Sox2 is indicated by *P* values ($-\log_{10}p$) on the *y*-axis, and the regions in which *p* values are $<10^{-10}$ are shown as green bars. Genomic sequence conservation is depicted by the graph showing homology between the mouse and human genomes. Two highly conserved regions upstream of the *Hes5* gene corresponded to the positions of the binding sites (arrowheads). ***D***, Genomic sequences of the mouse *Hes5* DRE and proximal promoter. Sox21-, Sox2-, CSL-, and POU-binding motifs were present in both regions. ***E***, ChIP–quantitative PCR assay using rat AHP cells. Immunoprecipitated *Hes5* DRE or proximal promoter fragments were quantified using the cycle threshold (Ct) values, which were normalized to the Ct of the input DNA. The binding of Sox21 or Sox2 to the DNA was determined by the fold relationship of enrichment of the target fragments in the ChIP DNA over the internal *Gapdh* gene. Data represent the mean ± SE. $^{*}p < 0.05$; $^{**}p < 0.01$ (two-sided *t* test). $n = 3$ for Sox21; $n = 4$ for Sox2.

Sox21, Sox2 did not modulate NICD-dependent luciferase activity (Fig. 8*D*) or cancel the repressive effect of Sox21 on the *Hes5* promoter, regardless of the dose of Sox2 expression vector used (Fig. 8*E*). These results suggest that Sox21 determines the expression level of *Hes5* in adult hippocampal NS/PCs independently of Sox2.

To further examine the effect of Sox21 on *Hes5* gene expression in adult NS/PCs, *Hes5* mRNA levels were analyzed in gain- and loss-of-function experiments. Endogenous *Hes5* gene expression in AHP cells was significantly decreased by retrovirally introduced Sox21 (Fig. 9*A*). By contrast, the endogenous *Hes5* expression level in the hippocampus of adult *Sox21*$^{-/-}$ mice was significantly higher than that in wild-type mice (Fig. 9*B*). Together, these results suggest that Sox21 acts as a transcriptional repressor of *Hes5* in adult hippocampal NS/PCs.

Sox21 regulates adult neurogenesis by repressing *Hes5* expression

To confirm the repressive role of Sox21 in *Hes5* expression *in vivo*, we analyzed the expression patterns of Sox21 and Hes5 in the adult DG using *Hes5*-NLS*lacZ* knock-in mice (Imayoshi et al., 2010). In the DG of *Hes5*-NLS*lacZ* knock-in adult mice, we observed LacZ-positive cells that expressed GFAP (Fig. 10*A*), and only 23.6% of Sox21-expressing cells demonstrated LacZ expression. Consistent with the restricted expression of Sox21 in type 1 and type 2a cells (Fig. 2), Sox21 and LacZ double-positive cells with or without type 1 cell-like fibers expressed GFAP, whereas none expressed PSA-NCAM (Fig. 10*B*). These results suggested that Sox21 and Hes5 were expressed in the adult DG in an essentially exclusive manner, although Hes5 may not be fully repressed by Sox21 in type 1 cells and in a portion of type 2a cells at the stage before transition to type 2b cells.

To address whether Hes5 regulates neurogenesis downstream of Sox21, we first examined the effect of reduced Hes5 expression on neuronal differentiation in the adult DG. We performed *Hes5* knockdown experiments *in vivo* by administering a *Hes5*-specific shRNA-expressing retrovirus (Fig. 11*A*) to the adult DG. *Hes5* knockdown in the DG resulted in a significant increase in the number of NeuN-positive cells compared with that in the control shRNA group (Fig. 11*B–D*). Like the previously reported anti-neurogenic function of Hes5 in embryonic NS/PCs (Ohtsuka et al., 1999), this result indicates that Hes5 is critical for the maintenance of the undifferentiated status of NS/PCs in the adult DG.

Finally, to investigate whether Hes5 is indeed a downstream effector of Sox21 in the regulation of adult hippocampal neuro-

Table 1. Candidate target genes of Sox21 and Sox2

Sox21 ChIP sequencing					Sox2 ChIP sequencing				
Accession No	Gene	Peak location	*p*	Overlap	Accession No	Gene	Peak location	*p*	Overlap
NM_177753	Sox21	0–5 kb down	110.2	+	NM_025434	Mrps28	Other intron	76.5	+
NM_025434	Mrps28	Other intron	82.2	+	NM_177753	Sox21	0–5 kb down	66.1	+
NM_172990	Pank4	10 k–5 kb up	79.8	+	NM_019514	Trim32	Other intron	56.7	−
NM_010419	Hes5	0–300 b up	79.8	+	NM_010308	Gnao1	Other intron	52.8	+
NM_008972	Ptma	0–300 b up	72.6	−	NM_178642	Tmem16a	Other intron	50.8	+
NM_175274	Ttyh3	10 k–5 kb down	71.8	+	NM_020296	Rbms1	Other intron	50.3	+
NM_008494	Lfng	1st intron	71.8	+	NM_023049	Asb2	10 k–5 kb down	44.4	+
NM_027268	Scrn1	1st intron	70.2	+	NM_010919	Nkx2–2	1 k–5 kb up	44.4	−
NM_001029850	Magi1	Other intron	69.4	+	NM_011137	Pou2f1	1st intron	44.4	+
NM_010439	Hmgb1	0–300 b up	66.9	−	NM_021458	Fzd3	1st intron	42.4	+
NM_011319	Sars	Other intron	63.9	+	NM_028778	Nuak2	1st intron	42.4	+
NM_010898	Nf2	0–300 b up	63.9	−	NM_008952	Pipox	0–300 b up	41.4	+
NM_011137	Pou2f1	1st intron	62.3	+	NM_172913	Tnrc9	0–5 kb down	40.9	−
NM_011817	Gadd45g	0–300 b up	62.3	−	NM_007434	Akt2	Other intron	39.5	−
NM_028778	Nuak2	1st intron	57.5	+	NM_008494	Lfng	1st intron	39.5	+
NM_001039484	Kcnj10	1st intron	55.9	−	NM_175274	Ttyh3	10 k–5 kb down	39.5	+
NM_146057	Dap	0–300 b up	55.1	−	NM_183144	Inpp5a	Other intron	38.5	+
NM_029756	Sdccag8	300–1 kb up	54.3	−	NM_001025074	Ntrk2	Other intron	38.0	+
NM_201610	Neil2	0–5 kb down	54.3	+	NM_027216	Slc39a11	Other intron	38.0	+
NM_010308	Gnao1	Other intron	54.3	+	NM_028263	Fgfbp3	10 k–5 kb down	37.5	−
NM_010191	Fdft1	0–300 b up	54.3	+	NM_201357	Tssc1	Other intron	37.0	+
NM_008997	Rab11b	0–300 b up	53.5	−	NM_027268	Scrn1	1st intron	36.5	+
NM_201357	Tssc1	Other intron	52.7	+	NM_010097	Sparcl1	1st intron	36.0	+
NM_025980	Nrarp	0–300 b up	52.7	−	NM_011936	Fto	1st intron	35.5	−
NM_013827	Mtf2	0–300 b up	51.9	−	NM_172544	Nrxn3	Other intron	35.5	+
NM_174988	Cdh22	Other intron	51.1	−	NM_007458	Ap2a1	10 k–5 kb down	34.5	−
NM_008629	Msi1	Other intron	50.3	−	BC057127	Fuz	10 k–5 kb up	34.5	−
AK163963	Gm1967	1st intron	50.3	+	NM_029365	Med25	300–1 kb up	34.5	−
NM_010913	Nfya	0–300 b up	49.5	−	NM_054043	Msi2	Other intron	34.5	+
NM_009694	Apobec2	10 k–5 kb down	49.5	−	NM_009846	Cd24a	1st intron	33.5	+
NM_207219	AI314976	0–300 b up	49.5	−	NM_016968	Olig1	10 k–5 kb up	33.5	−
NM_178642	Tmem16a	Other intron	48.7	+	NM_011319	Sars	Other intron	33.5	+
NM_198247	Sertad4	10 k–5 kb down	48.7	−	NM_178765	5730410E15Rik	Other intron	33.0	−
NM_020296	Rbms1	Other intron	48.7	+	NM_010419	Hes5	0–300 b up	33.0	+
NM_054043	Msi2	Other intron	48.7	+	NM_027032	Pacrg	Other intron	33.0	+
NM_011544	Tcf12	Other intron	47.9	−	NM_172990	Pank4	1 k–5 kb up	33.0	+
NM_010952	Oaz2	0–300 b up	47.9	−	NM_027504	Prdm16	Other intron	33.0	−
NM_026201	Ccar1	0–300 b up	47.9	−	NM_027539	Dcamkl2	Other intron	32.6	−
NM_181585	Pik3r3	300–1 kb up	46.3	−	NM_177618	BC030477	1st intron	31.6	+
NM_026272	Narf	0–300 b up	46.3	−	NM_172522	Megf11	Other intron	31.6	+
NM_016701	Nes	Other intron	43.1	+	NM_016701	Nes	Other intron	27.6	+

The 284 sites from the Sox21 ChIP sequencing data and the 301 sites from the Sox2 ChIP sequencing data were determined as described in Materials and Methods. Genes with these binding sites near their TSSs were annotated as bound genes and are shown here in decreasing order of maximum *p* values ($-\log_{10}p$). The top 40 genes and the *Nestin* gene are listed. The peak location is displayed relative to the genomic distance from the TSS. up, Upstream of TSS; down, downstream of TSS. If the peak resided within a coding region, the location is described as the 5′ UTR or introns. A plus sign in the Overlap column indicates that the gene in question was listed as both a Sox21 and Sox2 candidate target gene. The *Nestin* gene, which is expressed in NS/PCs, was bound by Sox2, consistent with a previous report showing that Sox2 binds to the second intron of the *Nestin* gene to modulate its expression (Zimmerman et al., 1994).

genesis, we examined whether *Hes5* overexpression was capable of canceling the neurogenic function of Sox21. Simultaneous expression of both proteins in NS/PCs *in vivo* was achieved by transducing cells with a construct containing Sox21 and Hes5 fused to a self-cleaving 2A peptide. Interestingly, compared with cells overexpressing *Sox21* alone, the proportion of NeuN-positive cells was dramatically reduced in cells overexpressing both *Sox21* and *Hes5* (Fig. 6*E*,*F*). This result clearly indicates an antagonistic effect of Hes5 on Sox21 in the context of adult neurogenesis in the DG.

Discussion

The present study provides evidence for a Sox21-mediated novel regulatory mechanism during adult neurogenesis in the DG. Sox21 represses the transcription of *Hes5* by binding to the DRE in the *Hes5* gene. *Hes5* repression by Sox21 is a vital event directing the neuronal differentiation of NS/PCs.

Essential role of Sox21 during adult neurogenesis

In the present study, we demonstrated that Sox21 was expressed in type 1 stem-like cells and type 2a progenitors in the adult hippocampal DG (Fig. 2). Our *in vivo* analysis of *Sox21*$^{-/-}$ mice revealed the expansion of type 2a cells and the reduction of type 2b cells (Fig. 4, 5). Moreover, we found that exogenous expression of Sox21 promoted neuronal differentiation in the DG. These findings lead to the conclusion that the major function of Sox21 is to drive the progression of progenitors toward differentiation, and that Sox21 exerts this function principally when NS/PCs are in the type 2a cell stage in the adult hippocampal DG.

Previous studies indicate that Ascl1 (Pleasure et al., 2000) and Ngn2 (Galichet et al., 2008) are factors that determine differentiation in embryonic DG morphogenesis. The neurogenic functions of Ascl1 and Ngn2 are predicted to be conserved in adult hippocampal neurogenesis due to their continued expression in the adult DG (Kim et al., 2007; Ozen et al., 2007). However, this

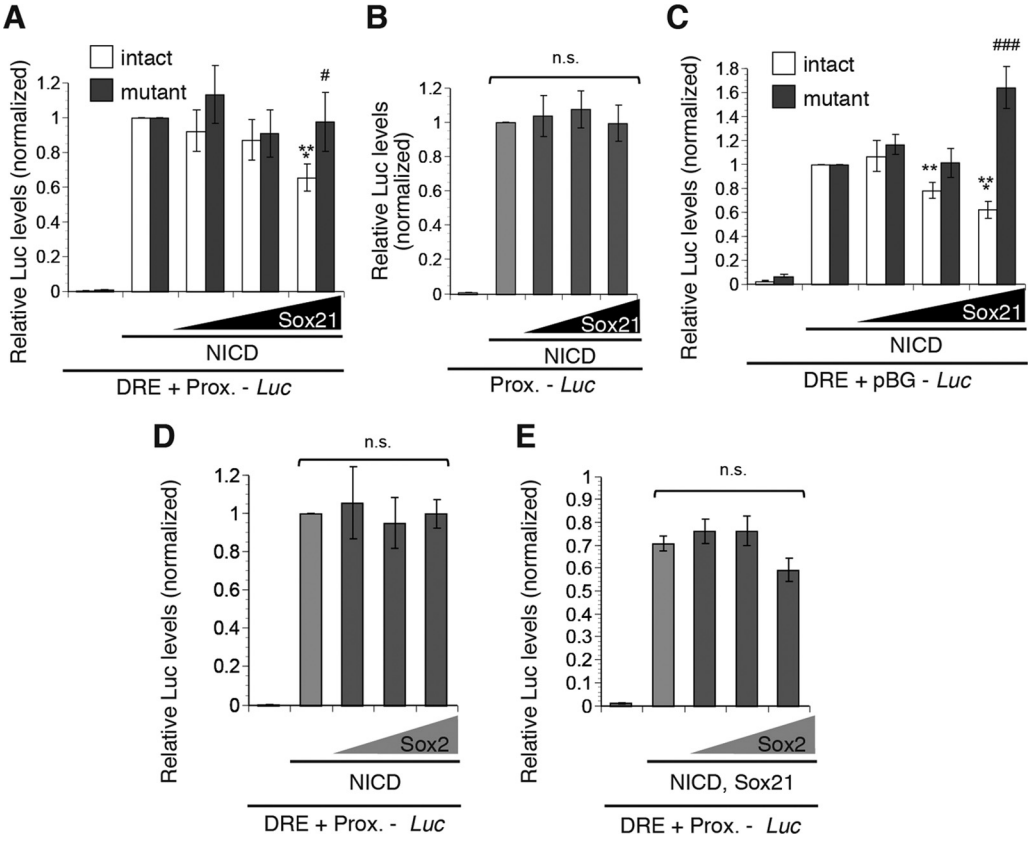

Figure 8. Repression of *Hes5* gene promoter activity by Sox21 but not Sox2. AHP cells were transfected with *Hes5* promoter–luciferase reporter constructs (1 μg per well) with or without expression vectors for *NICD*, *Sox21*, and/or *Sox2*. The histogram shows the ratio of firefly luciferase to that in cells transfected with the reporter construct and the *NICD*-expressing vector. The transfection efficiency was normalized to Renilla luciferase activity. ***A***, ***B***, The *Hes5* DRE and proximal promoter (−2767 to +73 bp from TSS) and the proximal promoter alone (−687 to +73 bp) were used as reporter constructs in ***A*** and ***B***, respectively. The open columns in ***A*** show the relative luciferase activities using the intact reporter construct, and the closed columns reflect the construct mutagenized at the Sox-binding sequence of the DRE (ACAAAGG to AagcttG). *NICD*-expression vector, 0.1 μg per well; *Sox21*-expression vector, 0.0001, 0.001, and 0.01 μg per well. ***C***, The *Hes5* DRE (−2676 to −2244 bp) combined with the β-globin minimal promoter was used. The open columns indicate the intact reporter construct, and the closed columns indicate the mutagenized construct as shown in ***A***. NICD, 1 μg per well; Sox21, 0.0001, 0.001, and 0.01 μg per well. ***D***, ***E***, The *Hes5* DRE and proximal promoter were used. ***D***, NICD, 0.1 μg per well, Sox2, 0.0001, 0.001, and 0.01 μg per well. ***E***, NICD, 0.1 μg per well; Sox21, 0.01 μg per well; Sox2, 0.0001, 0.001, and 0.01 μg per well. Data represent the mean ± SE. Statistical significance versus the intact promoter was assessed by two-sided *t* test ($n > 4$). $^{**}p < 0.01$, $^{***}p < 0.001$ versus NICD alone; $^{\#}p < 0.05$; $^{\#\#\#}p < 0.001$ versus intact promoter. n.s., No significance versus NICD and Sox21 alone according to the two-sided *t* test ($n > 4$). Prox., Proximal promoter.

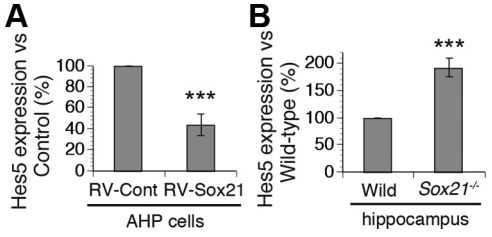

Figure 9. Repressive role of Sox21 in *Hes5* expression *in vitro* and *in vivo*. ***A***, *In vitro* analysis of *Hes5* expression level confirmed by RT-qPCR. AHP cells infected with a *Sox21*-expressing retrovirus (RV-Sox21) expressed *Hes5* at a lower level than controls (RV-Cont). $^{***}p < 0.001$ (two-sided *t* test). $n = 5$. ***B***, Endogenous *Hes5* expression level in 6-week-old wild-type and *Sox21*$^{-/-}$ hippocampus determined using RT-qPCR. $^{***}p < 0.001$ versus wild-type mice (two-sided *t* test). $n = 4$. Data represent the mean ± SE.

hypothesis is controversial because Ascl1 overexpression in adult DG was reported to redirect the fate of NS/PCs into oligodendrocyte lineage (Jessberger et al., 2008). Here, we present the first evidence from both *in vivo* loss- and gain-of-function experiments showing that a single transcription factor, Sox21, can govern the transition of progenitors into neuronal differentiation stages in the adult hippocampus.

The generation of new neurons was significantly abrogated in *Sox21*$^{-/-}$ mice; however, hippocampal neurogenesis was not completely abolished (Fig. 4). This observation may be attributable to the existence of some NS/PCs that pursue their neurogenic steps in a Sox21-independent manner, judging from the existence of Sox21-negative NS/PCs in the DG (Fig. 2). Moreover, other factors in addition to Sox21 may play a role in *Hes5* gene repression. For example, the Cdc42–mammalian target of rapamycin pathway (Endo et al., 2009) and Fezf proteins (Shimizu et al., 2010) control the neuronal differentiation of NS/PCs by repressing the *Hes5* gene. These signaling pathways may have compensated for the loss of Sox21 by repressing *Hes5* transcription.

Sox21-mediated regulation of *Hes5* expression in NS/PCs

In the adult mammalian brain, Notch signaling is involved in the maintenance of NS/PCs, and the conditional knock-out of CSL forces NS/PCs to differentiate into neurons (Imayoshi et al., 2010). Likewise, the abrogation of Notch signaling leads to the precocious transition of NS/PCs into neurons in the adult hippocampal DG, and overexpression of *NICD* induces the expansion of the highly proliferative NS/PC population (Breunig et al., 2007). Hes5 is a canonical downstream effector of Notch signal-

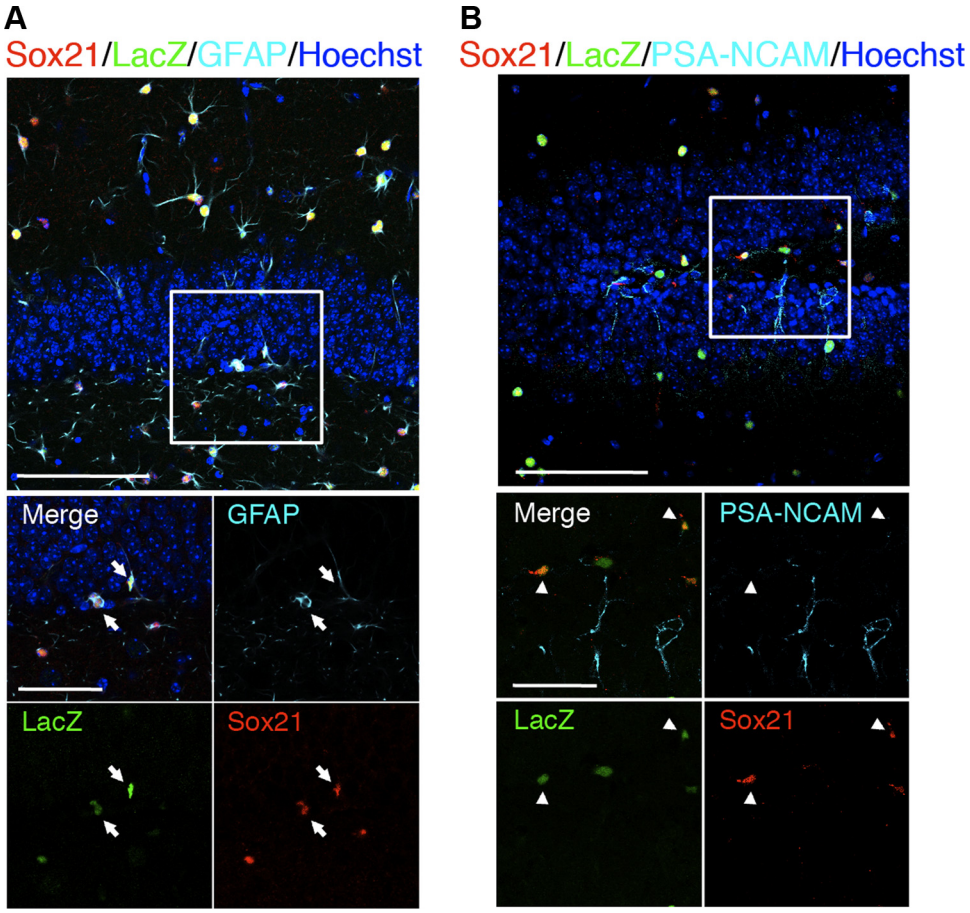

Figure 10. Colocalization of Sox21 and Hes5 in a small portion of NS/PCs, but not in immature neurons. ***A***, ***B***, Triple immunohistochemical analyses of Hes5 expression in the adult DG using *Hes5*-NLS*lacZ* knock-in mice. ***A***, Triple staining for Sox21, Hes5 (lacZ), and the NS/PC marker GFAP. Arrows indicate Sox21+/Hes5+/GFAP+ cells. ***B***, Triple staining for Sox21, Hes5, and the immature neuronal marker PSA-NCAM. Arrowheads indicate Sox21+/Hes5+/PSA-NCAM cells. Scale bars: top row, 100 μm; magnified, 50 μm.

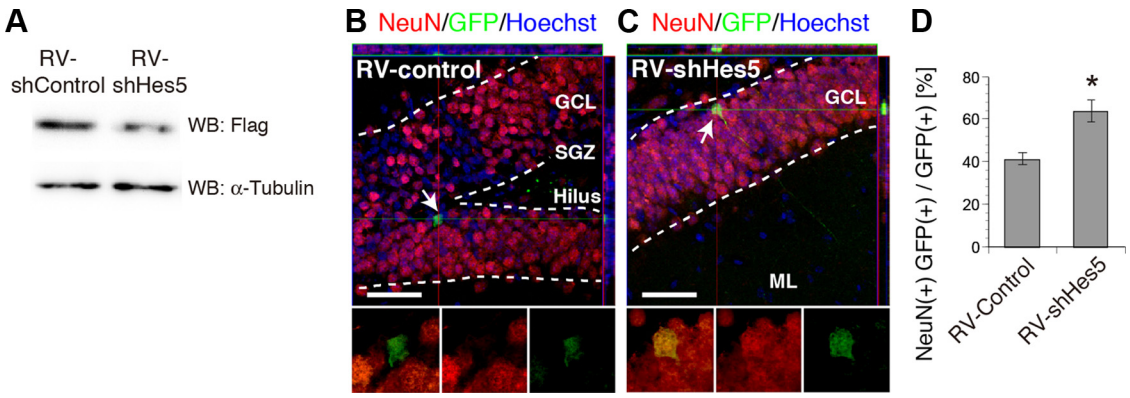

Figure 11. Suppression of Hes5 expression promoted neuronal differentiation in the adult DG. ***A***, Western blotting to validate *Hes5* shRNA. NIH3T3 cells stably expressing FLAG-Hes5 were infected with a retrovirus encoding control shRNA (RV-shControl) or *Hes5* shRNA (RV-shHes5) for 7 d. α-Tubulin expression was used as an internal control. ***B***, ***C***, Micrographs of retrovirus-labeled GFP+ newborn cells (arrows) at 21 d after retrovirus infusion into the DG of 6-week-old wild-type mice. Control shRNA-overexpressing (***B***) and *Hes5* shRNA-overexpressing (***C***) groups are shown. The GFP-positive infected cells in ***C*** demonstrated NeuN expression. ***D***, Quantification of the neuronal differentiation of newborn cells at 21 d after retrovirus injection. Newborn neurons were identified by the presence of NeuN expression, and the data are expressed as the proportion of NeuN+ cells among the total GFP+ infected cell population in the SGZ and GCL. Data represent the mean ± SE. $^*p < 0.05$ (two-sided *t* test). $n = 4$. Scale bars: 50 μm.

ing (Ohtsuka et al., 1999), which inhibits neuronal differentiation by repressing proneural genes such as *Mash1*, *Math*, and *Neurogenin* (Kageyama et al., 2005), and is believed to be involved in the maintenance of the undifferentiated status of NS/PCs in the adult DG (Lugert et al., 2010). *Hes5* expression is mainly activated by binding of the CSL transcription factor to the *Hes5* proximal promoter (Takebayashi et al., 1995; Ong et al., 2006). However, because of the existence of Sox-binding elements in the *Hes5* promoter, Sox family proteins are also predicted to control *Hes5* expression (Takanaga et al., 2009). To the best of our knowledge, the present study is the first to show that Sox21 binds to the *Hes5* gene and represses its transcription (Figs. 7–9). Furthermore, the

repressive effect of Sox21 was blocked by introducing a mutation into the Sox-binding site in a novel distal *Hes5* regulatory element (Fig. 8), suggesting that Sox21 may negatively regulate Notch-downstream signaling via a Notch/CSL-independent pathway. Furthermore, we showed that the Sox21-mediated repression of *Hes5* was sufficient to allow the neuronal differentiation of NS/PCs in the adult DG (Fig. 6). Interestingly, the *Hes5* proximal promoter was not responsible for the Sox21-mediated regulation of *Hes5* transcription, implying that the DRE plays a notable role in the progression of adult neurogenesis.

Although our motif analyses revealed the possibility that Sox21 and Sox2 proteins recognize *cis*-elements in a similar way (Fig. 7*B*), only 97 genomic loci (34.5% of the loci bound by Sox21 and 32.2% of the loci bound by Sox2) turned out to be bound by both Sox21 and Sox2 (Fig. 7*A*). Furthermore, regulation of *Hes5* gene expression differed between these Sox proteins: Sox21, but not Sox2, bound to the *Hes5* DRE. The fact that Sox2 did not bind to the *Hes5* DRE may explain why Sox2 did not antagonize Sox21 in the regulation of *Hes5* gene expression. To our knowledge, this is the first example of competition between SoxB1 and SoxB2 proteins. To better understand this phenomenon, it would be interesting to identify the transcriptional factor complex recruited by Sox21. The presence of the conserved POU3f2 (Brn2) octamer sequence close to the Sox motif in the *Hes5* DRE (Fig. 7*D*) implies that Brn2 may participate in regulating *Hes5* expression through Sox21. The fact that Sox2 and Brn2 synergistically regulate *Nestin* gene expression by binding to adjacent Sox- and POU-binding motifs, respectively (Zimmerman et al., 1994; Tanaka et al., 2004), supports the idea of interplay between Sox protein and Brn2.

From the finding that simultaneous overexpression of *Hes5* and *Sox21* in the adult DG blocked the neuronal differentiation induced by retrovirus-delivered Sox21 (Fig. 6*E*,*F*), we concluded that the *Hes5* gene is a functional downstream target of Sox21. However, the involvement of other possible target genes in the progression of Sox21-induced neuronal differentiation cannot be excluded. ChIP sequencing results identified other candidate genes likely related to brain development. For example, Sox21 seems to bind to the intronic region of the *Msi1* ($-\mathrm{Log}_{10}p = 50.3$) and *Msi2* genes ($-\log_{10}p = 48.7$) (Table 1). Musashi-1 is highly expressed in NS/PCs in the mammalian CNS (Sakakibara et al., 1996; Tonchev et al., 2005) and is thought to contribute to NS/PC self-renewal (Okano et al., 2005) and hippocampal adult neurogenesis (Kempermann et al., 2006). It would be of interest to examine the role of Sox21 in the transcriptional regulation of *Msi1*.

Furthermore, the ChIP sequencing results revealed that Sox21 may bind to genes related to Notch signaling: for example, the *Lfng* gene, which encodes Lunatic fringe protein ($-\log_{10}p = 71.8$), and the *Pou2f1* (*Oct1*) gene ($-\log_{10}p = 62.3$) (Table 1). *Lfng* expression is restricted to the ventricular zone of developing cortical walls in mice (Ishii et al., 2000) and potentiates Dll-1-mediated Notch signaling to maintain the proliferation of NS/PCs (Kato et al., 2010). *Pou2f1* expression is reportedly induced by NICD and is required for radial glia formation in the *Xenopus* hindbrain (Kiyota et al., 2008). Intriguingly, Sox21 tends to enhance the expression of *Lfng* and suppress *Pou2f1* expression in AHP cells (our unpublished results). Although the detailed expression profiles of *Lfng* and *Pou2f1* in the adult brain, and their roles in regulating hippocampal adult neurogenesis, remain unknown, Sox21 may exert its neurogenic function by determining the optimal level of Notch signaling transduction by controlling these Notch-related factors.

This study demonstrated that Sox21 regulates adult neurogenesis *in vivo* and contributes to the generation of new neurons. Recently, increasing evidence has revealed a profound relationship between adult neurogenesis and learning (Shors et al., 2001), depression (Malberg et al., 2000), and some neurodegenerative diseases, including Huntington's disease (Curtis et al., 2003), Parkinson's disease (Winner et al., 2004), and Alzheimer's disease (Wen et al., 2004; Donovan et al., 2006). It is therefore of great value to focus on the involvement of Sox21 in the physiology of brain function as well as the pathophysiology of such diseases. Identifying targets other than *Hes5* using our genomewide ChIP sequencing information should help to increase the current understanding of the gene network that controls adult neurogenesis.

References

Akazawa C, Sasai Y, Nakanishi S, Kageyama R (1992) Molecular characterization of a rat negative regulator with a basic helix-loop-helix structure predominantly expressed in the developing nervous system. J Biol Chem 267:21879–21885.

Bailey TL, Elkan C (1994) Fitting a mixture model by expectation maximization to discover motifs in biopolymers. Proc Int Conf Intell Syst Mol Biol 2:28–36.

Bani-Yaghoub M, Tremblay RG, Lei JX, Zhang D, Zurakowski B, Sandhu JK, Smith B, Ribecco-Lutkiewicz M, Kennedy J, Walker PR, Sikorska M (2006) Role of Sox2 in the development of the mouse neocortex. Dev Biol 295:52–66.

Breunig JJ, Silbereis J, Vaccarino FM, Sestan N, Rakic P (2007) Notch regulates cell fate and dendrite morphology of newborn neurons in the postnatal dentate gyrus. Proc Natl Acad Sci U S A 104:20558–20563.

Curtis MA, Penney EB, Pearson AG, van Roon-Mom WM, Butterworth NJ, Dragunow M, Connor B, Faull RL (2003) Increased cell proliferation and neurogenesis in the adult human Huntington's disease brain. Proc Natl Acad Sci U S A 100:9023–9027.

Donovan MH, Yazdani U, Norris RD, Games D, German DC, Eisch AJ (2006) Decreased adult hippocampal neurogenesis in the PDAPP mouse model of Alzheimer's disease. J Comp Neurol 495:70–83.

Duan X, Kang E, Liu CY, Ming GL, Song H (2008) Development of neural stem cell in the adult brain. Curr Opin Neurobiol 18:108–115.

Endo M, Antonyak MA, Cerione RA (2009) Cdc42-mTOR signaling pathway controls Hes5 and Pax6 expression in retinoic acid-dependent neural differentiation. J Biol Chem 284:5107–5118.

Gage FH (2000) Mammalian neural stem cells. Science 287:1433–1438.

Galichet C, Guillemot F, Parras CM (2008) Neurogenin 2 has an essential role in development of the dentate gyrus. Development 135:2031–2041.

Hodge RD, Kowalczyk TD, Wolf SA, Encinas JM, Rippey C, Enikolopov G, Kempermann G, Hevner RF (2008) Intermediate progenitors in adult hippocampal neurogenesis: Tbr2 expression and coordinate regulation of neuronal output. J Neurosci 28:3707–3717.

Imaizumi Y, Sakaguchi M, Morishita T, Ito M, Poirier F, Sawamoto K, Okano H (2011) Galectin-1 is expressed in early-type neural progenitor cells and down-regulates neurogenesis in the adult hippocampus. Mol Brain 4:7.

Imayoshi I, Sakamoto M, Yamaguchi M, Mori K, Kageyama R (2010) Essential roles of Notch signaling in maintenance of neural stem cells in developing and adult brains. J Neurosci 30:3489–3498.

Ishii Y, Nakamura S, Osumi N (2000) Demarcation of early mammalian cortical development by differential expression of fringe genes. Brain Res Dev Brain Res 119:307–320.

Jessberger S, Toni N, Clemenson GD Jr, Ray J, Gage FH (2008) Directed differentiation of hippocampal stem/progenitor cells in the adult brain. Nat Neurosci 11:888–893.

Kageyama R, Ohtsuka T, Hatakeyama J, Ohsawa R (2005) Roles of bHLH genes in neural stem cell differentiation. Exp Cell Res 306:343–348.

Kan L, Israsena N, Zhang Z, Hu M, Zhao LR, Jalali A, Sahni V, Kessler JA (2004) Sox1 acts through multiple independent pathways to promote neurogenesis. Dev Biol 269:580–594.

Kaneshiro K, Tsutsumi S, Tsuji S, Shirahige K, Aburatani H (2007) An integrated map of p53-binding sites and histone modification in the human ENCODE regions. Genomics 89:178–188.

Kato TM, Kawaguchi A, Kosodo Y, Niwa H, Matsuzaki F (2010) Lunatic

fringe potentiates Notch signaling in the developing brain. Mol Cell Neurosci 45:12–25.
Kel AE, Gössling E, Reuter I, Cheremushkin E, Kel-Margoulis OV, Wingender E (2003) MATCH: A tool for searching transcription factor binding sites in DNA sequences. Nucleic Acids Res 31:3576–3579.
Kempermann G, Jessberger S, Steiner B, Kronenberg G (2004) Milestones of neuronal development in the adult hippocampus. Trends Neurosci 27:447–452.
Kempermann G, Chesler EJ, Lu L, Williams RW, Gage FH (2006) Natural variation and genetic covariance in adult hippocampal neurogenesis. Proc Natl Acad Sci U S A 103:780–785.
Kim EJ, Leung CT, Reed RR, Johnson JE (2007) *In vivo* analysis of Ascl1 defined progenitors reveals distinct developmental dynamics during adult neurogenesis and gliogenesis. J Neurosci 27:12764–12774.
Kiso M, Tanaka S, Saba R, Matsuda S, Shimizu A, Ohyama M, Okano HJ, Shiroishi T, Okano H, Saga Y (2009) The disruption of Sox21-mediated hair shaft cuticle differentiation causes cyclic alopecia in mice. Proc Natl Acad Sci U S A 106:9292–9297.
Kitamura T, Koshino Y, Shibata F, Oki T, Nakajima H, Nosaka T, Kumagai H (2003) Retrovirus-mediated gene transfer and expression cloning: powerful tools in functional genomics. Exp Hematol 31:1007–1014.
Kiyota T, Kato A, Altmann CR, Kato Y (2008) The POU homeobox protein Oct-1 regulates radial glia formation downstream of Notch signaling. Dev Biol 315:579–592.
Lathia JD, Mattson MP, Cheng A (2008) Notch: from neural development to neurological disorders. J Neurochem 107:1471–1481.
Lefebvre V, Dumitriu B, Penzo-MéndezA, Han Y, Pallavi B (2007) Control of cell fate and differentiation by Sry-related high-mobility-group box (Sox) transcription factors. Int J Biochem Cell Biol 39:2195–2214.
Lewis J (1996) Neurogenic genes and vertebrate neurogenesis. Curr Opin Neurobiol 6:3–10.
Lugert S, Basak O, Knuckles P, Haussler U, Fabel K, Götz M, Haas CA, Kempermann G, Taylor V, Giachino C (2010) Quiescent and active hippocampal neural stem cells with distinct morphologies respond selectively to physiological and pathological stimuli and aging. Cell Stem Cell 6:445–456.
Malberg JE, Eisch AJ, Nestler EJ, Duman RS (2000) Chronic antidepressant treatment increases neurogenesis in adult rat hippocampus. J Neurosci 20:9104–9110.
Ohba H, Chiyoda T, Endo E, Yano M, Hayakawa Y, Sakaguchi M, Darnell RB, Okano HJ, Okano H (2004) Sox21 is a repressor of neuronal differentiation and is antagonized by YB-1. Neurosci Lett 358:157–160.
Ohtsuka T, Ishibashi M, Gradwohl G, Nakanishi S, Guillemot F, Kageyama R (1999) Hes1 and Hes5 as notch effectors in mammalian neuronal differentiation. EMBO J 18:2196–2207.
Okano H, Kawahara H, Toriya M, Nakao K, Shibata S, Imai T (2005) Function of RNA-binding protein Musashi-1 in stem cells. Exp Cell Res 306:349–356.
Ong CT, Cheng HT, Chang LW, Ohtsuka T, Kageyama R, Stormo GD, Kopan R (2006) Target selectivity of vertebrate notch proteins. Collaboration between discrete domains and CSL-binding site architecture determines activation probability. J Biol Chem 281:5106–5119.
Ozen I, Galichet C, Watts C, Parras C, Guillemot F, Raineteau O (2007) Proliferating neuronal progenitors in the postnatal hippocampus transiently express the proneural gene Ngn2. Eur J Neurosci 25:2591–2603.
Palmer TD, Takahashi J, Gage FH (1997) The adult rat hippocampus contains primordial neural stem cells. Mol Cell Neurosci 8:389–404.
Pleasure SJ, Collins AE, Lowenstein DH (2000) Unique expression patterns of cell fate molecules delineate sequential stages of dentate gyrus development. J Neurosci 20:6095–6105.
Sakaguchi M, Shingo T, Shimazaki T, Okano HJ, Shiwa M, Ishibashi S, Oguro H, Ninomiya M, Kadoya T, Horie H, Shibuya A, Mizusawa H, Poirier F, Nakauchi H, Sawamoto K, Okano H (2006) A carbohydrate-binding protein, Galectin-1, promotes proliferation of adult neural stem cells. Proc Natl Acad Sci U S A 103:7112–7117.
Sakakibara S, Imai T, Hamaguchi K, Okabe M, Aruga J, Nakajima K, Yasutomi D, Nagata T, Kurihara Y, Uesugi S, Miyata T, Ogawa M, Mikoshiba K, Okano H (1996) Mouse-Musashi-1, a neural RNA-binding protein highly enriched in the mammalian CNS stem cell. Dev Biol 176:230–242.
Sandberg M, Källström M, Muhr J (2005) Sox21 promotes the progression of vertebrate neurogenesis. Nat Neurosci 8:995–1001.
Seri B, García-Verdugo JM, McEwen BS, Alvarez-Buylla A (2001) Astrocytes give rise to new neurons in the adult mammalian hippocampus. J Neurosci 21:7153–7160.
Shimizu T, Nakazawa M, Kani S, Bae YK, Shimizu T, Kageyama R, Hibi M (2010) Zinc finger genes Fezf1 and Fezf2 control neuronal differentiation by repressing Hes5 expression in the forebrain. Development 137:1875–1885.
Shors TJ, Miesegaes G, Beylin A, Zhao M, Rydel T, Gould E (2001) Neurogenesis in the adult is involved in the formation of trace memories. Nature 410:372–376.
Suh H, Consiglio A, Ray J, Sawai T, D'Amour KA, Gage FH (2007) *In vivo* fate analysis reveals the multipotent and self-renewal capacities of Sox2+ neural stem cells in the adult hippocampus. Cell Stem Cell 1:515–528.
Tada H, Ishii S, Kimura H, Hattori H, Okada Y, Suzuki N, Okano HJ (2007) Identification and evaluation of high-titer anti-Sox Group B antibody in limbic encephalitis. Inflamm Regen 27:37–44.
Takanaga H, Tsuchida-Straeten N, Nishide K, Watanabe A, Aburatani H, Kondo T (2009) Gli2 is a novel regulator of sox2 expression in telencephalic neuroepithelial cells. Stem Cells 27:165–174.
Takebayashi K, Akazawa C, Nakanishi S, Kageyama R (1995) Structure and promoter analysis of the gene encoding the mouse helix-loop-helix factor HES-5. Identification of the neural precursor cell-specific promoter element. J Biol Chem 270:1342–1349.
Tanaka S, Kamachi Y, Tanouchi A, Hamada H, Jing N, Kondoh H (2004) Interplay of SOX and POU factors in regulation of the Nestin gene in neural primordial cells. Mol Cell Biol 24:8834–8846.
Tonchev AB, Yamashima T, Sawamoto K, Okano H (2005) Enhanced proliferation of progenitor cells in the subventricular zone and limited neuronal production in the striatum and neocortex of adult macaque monkeys after global cerebral ischemia. J Neurosci Res 81:776–788.
Wakabayashi K, Okamura M, Tsutsumi S, Nishikawa NS, Tanaka T, Sakakibara I, Kitakami J, Ihara S, Hashimoto Y, Hamakubo T, Kodama T, Aburatani H, Sakai J (2009) The peroxisome proliferator-activated receptor gamma/retinoid X receptor alpha heterodimer targets the histone modification enzyme PR-Set7/Setd8 gene and regulates adipogenesis through a positive feedback loop. Mol Cell Biol 29:3544–3555.
Wang TW, Stromberg GP, Whitney JT, Brower NW, Klymkowsky MW, Parent JM (2006) Sox3 expression identifies neural progenitors in persistent neonatal and adult mouse forebrain germinative zones. J Comp Neurol 497:88–100.
Wen PH, Hof PR, Chen X, Gluck K, Austin G, Younkin SG, Younkin LH, DeGasperi R, Gama Sosa MA, Robakis NK, Haroutunian V, Elder GA (2004) The presenilin-1 familial Alzheimer disease mutant P117L impairs neurogenesis in the hippocampus of adult mice. Exp Neurol 188:224–237.
Winner B, Lie DC, Rockenstein E, Aigner R, Aigner L, Masliah E, Kuhn HG, Winkler J (2004) Human wild-type alpha-synuclein impairs neurogenesis. J Neuropathol Exp Neurol 63:1155–1166.
Zimmerman L, Parr B, Lendahl U, Cunningham M, McKay R, Gavin B, Mann J, Vassileva G, McMahon A (1994) Independent regulatory elements in the nestin gene direct transgene expression to neural stem cells or muscle precursors. Neuron 12:11–24.